MINISTRY OF SUPPLY

AERONAUTICAL RESEARCH COUNCIL
CURRENT· PAPERS

An Investigation into the Pitot Rake Method of Measuring Turbo Jet Engine Thrust in Flight

By

Fl./Lt. J. Stephenson, B.Sc. R.N.Z.A.F.,
R. T. Shields, B.A.
and
D. W. Bottle, B.Sc.

ADDENDA

Summary

Main conclusions (3), after "7% lower than corresponding thrusts at 5,000 ft." add "at max. R.P.M.".

1. Introduction

Page 3, four lines from bottom delete "zero" substitute "ambient atmospheric".

Page 4, 7th line, delete "and".

5. Consideration of Combined Tests

Page 15, 5.1.1, (3) 2nd line, delete "altitude" substitute "attitude".

6. Conclusions

Page 19, 3rd paragraph, after "...... compared with 5,000 ft. of the order of 7%" add "at the maximum R.P.M. of the tests."

Appendix 1

Page 1, para. 2, equation (4), the expression in the square bracket should read:

$$\left[\left(\frac{P_5}{H_5}\right)^{\frac{1}{\gamma}} - \frac{P_5}{H_5}\right]$$

Page 2, para.3, 6th line, after "...... equation (2)" add "assuming no mixing losses".

`

AEROPLANE AND ARMAMENT EXPERIMENTAL ESTABLISHMENT

A.A.E.E |Res|265

An investigation into the pitot rake method of measuring turbo jet engine thrust in flight

by

Fl/Lt. J. Stephenson, B.Sc., R.N.Z.A.F.,
R. T. Shields, B.A.
and
D. W. Bottle, B.Sc.

Summary

Tests have been made to establish whether a pitot rake could be used as an absolute measure of the thrust of a jet engine on the ground and in flight.

The tests were made to investigate errors due to the assumptions inherent in the single pitot method of estimating thrust in flight, and to establish if a rake can be used to calibrate the single pitot of an uncalibrated engine installed in an aircraft. The tests were also planned to check the generally accepted non-dimensional thrust relationship for jet engines.

The tests were made on Derwent 5 engines installed in Meteor 4 aircraft. The tests covered a wide range of flight conditions and included test bed measurements on bare engines and later, measurements of exit static pressure. Although the tests could not all be made on the same engine, the same final nozzle was used in all the main tests.

The main conclusions were:-

(1)   Static tubes must be incorporated in the pitot rake to give absolute thrust measurements and even so a discrepancy of 2% requires further investigation.

(2)   The single pitot method of estimating flight thrust based on engine test bed calibration was in error by as much as 6% due to changes in total pressure sampled by the single pitot and in the magnitude of the exit static pressure between calibration and test conditions.

Using the pitot static rake to calibrate the single pitot of an installed engine introduced flight thrust errors no larger and possibly smaller.

(3)   Non-dimensional thrusts at 35,000 ft. were some 7% lower than corresponding thrusts at 5,000 ft.

Further tests are required to establish the magnitude of these effects on other engine types.

List of contents Page

List of tables

List of illustrations

1. Introduction

It is desirable in all flight performance tests on turbo jet aircraft to measure the engine thrust. This is required firstly to check that the engines are in flight developing the thrust which is expected, and secondly the thrust is required so that the aircraft drag can be obtained from the performance equation. Such routine thrust measurements are desirable because differences in thrust between nominally identical engines, and even differences in thrust during the life of a particular engine cannot be neglected.

The desirable requirements of any method of thrust measurement to be used at A. & A.E.E. are as follows (Ref.1).

(1) The installation must have a known or negligible effect on flight performance, since the performance of a standard aircraft is being dealt with.

(2) The method should have an accuracy of $\pm$ 1% if possible.

(3) The installation must be capable of retrospective embodiment, without major modification, in any type. Test bed calibration of an engine, as in the single pitot method, would come under the category of major modification, since test aircraft may arrive at this Establishment with an uncalibrated engine fitted.

(4) The additional instrumentation required should not preclude the use of the normal performance automatic observer in an aircraft in which space is limited.

(5) The method should preferably give a direct measurement of the gross thrust and not involve considerations of thrust on engine bearers, since retrospective embodiment would be very difficult and also accurate measurements of air intake efficiency would be necessary (Ref.2).

(6) It should if possible be suitable for use with reheat.

The normal method used to date to measure jet thrust in flight has been the well known "single pitot" method (Ref.3). This method meets requirements 1, 4 and 5, but it has the disadvantages firstly that its accuracy is not known precisely due to lack of information on the assumptions inherent in the method, and secondly that full test bed thrust calibrations are required for each engine used for performance flight tests.

To overcome these shortcomings of the single pitot method, it was decided to investigate the assumptions of the method, and to try to develop a simple method of calibrating the single pitot which would be independent of test bed measurements.

It will be convenient at this point to re-examine the basis of thrust measurement by momentum methods, and in particular point out the assumptions made in the single pitot method. This has been done more fully in Appendix 1 to which reference should be made for details.

The basic equation for nett thrust in flight is

$$X_N = - \frac{M_0 V_0}{g} + \frac{M_6 V_6}{g} + (P_6 - P_0) A_6 , \qquad \ldots\ldots(1)$$

where only the internal flow through the engine, M, is considered, and the plane 6 is chosen where the static pressure is zero for subsonic jets, or alternatively, where the throat occurs for supersonic jets. (Ref.4).

Similarly the gross thrust in flight, on the ground or on a test bed is given by

$$X = \frac{M_6 V_6}{g} + (P_6 - P_0) A_6 \qquad \ldots\ldots(2)$$

and for the test bed $X = X_T$ the thrust measured on the/thrust meter.

In flight it is necessary to make measurements at the jet exit in order to define the internal flow boundaries. Assuming that mixing losses between plane 5 and 6 are negligible the expression for gross thrust is then

$$X = \left\{ \frac{\rho_6 A_5 v_6^2}{g} + (P_6 - P_0) A_5 \right\} \times \frac{A_6}{A_5} \qquad \dots\dots\dots(3)$$

and all quantities in (3) can be calculated given the total and static pressure at the jet exit, and assuming isentropic flow from plane 5 to 6. Thrusts would be estimated from equation (3) from pitot static rake measurements.

If the assumption is made that $P_5 = P_6$ i.e. that the vena contracta or throat occurs at the jet exit,

$$\text{Then } X = \frac{M_5 V_5}{g} + (P_5 - P_0) A_5 \qquad \dots\dots\dots(4)$$

from which

$$\frac{X}{P_0 A_5} = F_1 \left(\frac{H_5}{P_0}\right) \qquad \dots\dots\dots(5)$$

where F_1 is known (see Equation 4 of Appendix 1)

Thrusts would be calculated from Equation 4 from measurements with a pitot rake.

In all equations (1) to (5) it is assumed that an integration over the internal flow cross section will be made if conditions are not uniform.

In the single pitot method a further assumption is made that

$$\frac{H_4}{H_5} = F_2 \left(\frac{H_4}{P_0}\right) \qquad \text{where } H_4 \text{ is the single pitot total pressure} \qquad \dots\dots\dots(6)$$

and combining (5) and (6) gives

$$\frac{X}{P_0 A_5} = F_3 \left(\frac{H_4}{P_0}\right) F_1 \left(\frac{H_4}{P_0}\right) \qquad \dots\dots\dots(7)$$

A test bed calibration provides measured values of $\frac{H_4}{P_0}$ and $\frac{X_T}{P_0} = \frac{X}{P_0}$ from which the effective area $A_f' = A_5 F_3 \left(\frac{H_4}{P_0}\right)$ is determined, and hence equation (7) is used to determine gross thrusts in flight.

To summarise, the assumptions in the single pitot method refer to flow conditions in the final nozzle exit and are:-

(1) The relation between $\frac{H_4}{P_0}$ and $\frac{H_5}{P_0}$ i.e. the total pressure distribution is the same on the test bed and in flight.

(2) The relation between $\frac{P_5}{P_0}$ and $\frac{H_4}{P_0}$, i.e. the final nozzle static pressure is also the same on the test bed and in flight.

(3) It is necessary to extrapolate values of A_f' obtained on the test bed to higher values of pressure ratio $\frac{H_4}{P_0}$ only obtainable in flight.

Measurements have therefore been made of total head distribution and static pressure in the final nozzle of Derwent 5 engines when installed in a Meteor 4 aircraft both on the ground and in flight, and also on the bare engine on the test bed. The measurements were made using pitot and pitot static rakes.

It was thought that if the rake method proved successful as an absolute measure of thrust, it could be used to calibrate the single pitot on the ground without need for test bed measurements. The tests were also designed to check how closely thrusts measured in flight by the rake, agreed with the generally assumed non-dimensional relationship.

The tests were first planned to investigate total head distribution changes using pitot rakes. The importance of the static pressure assumptions was realised later, and separate measurements of static pressures had to be made on another Meteor 4 aircraft. This has complicated the analysis of results.

In fact the tests made fell into the following three phases:-

Phase 1. **Engine in aircraft.** Tests to measure total pressure at the single pitot and pitot rake, both static on the ground and in flight.

Phase 2. **Engine on test bed.** Measurements of thrust by balance and of single pitot and pitot rake total pressure. This revealed a discrepancy between the thrust measured on the test bed balance and thrust calculated from the rake total pressure readings which was ascribed to the jet not being fully contracted at the final nozzle as is assumed conventionally in calculating thrust from pitot readings.

Phase 3. **Engine in aircraft.** As a result of/2, measurements were made of static pressure at the final nozzle repeating Phase 1 ground and flight test conditions. These values of static pressure enabled a correction to be applied to the thrust estimated from the pitot comb in Phase 1 tests.

Paragraphs 2, 3 and 4 describe in detail the tests in Phase 1, 2 and 3 respectively. The combined results are then discussed in paragraph 5.

2. **Phase 1 tests.** **Total head measurements engine installed in the aircraft**

The Phase 1 tests were undertaken to obtain a comparison between thrusts measured using single pitot with a test bed effective area calibration, and the thrust obtained directly from a total pressure traverse at the final nozzle exit using a pitot rake. The tests were also planned to give information on the suitability of calibrating a single pitot against a pitot rake during ground runs of an engine installed in an aircraft, and to check the validity of the non-dimensional relationship between non-dimensional thrust X/p and $N/\sqrt{\theta_1}$ by a comparison of thrusts measured over as wide a range of altitude as possible.

When the tests were started it was thought that flow distribution changes with variation in flight Mach number, Reynolds number and altitude would be the main source of error in thrust estimated from single pitot pressures and the tests were planned to show up such changes. It was later appreciated that departures in the static pressure at the final nozzle exit from the values normally assumed could not be neglected.

In this account of Phase 1 tests only measurements of total head will therefore be discussed, and the fully corrected thrusts estimated from the Phase 1 total head results and the static measurements of Phase 3 tests will be discussed in paragraph 5.

2.1 Description of aircraft

2.1.1 The aircraft used for the Phase 1 tests, Meteor RA.420, was a production short span Meteor F. Mk.4.

/The aircraft..

The aircraft was flown with a 180 gallon ventral tank fitted, at a normal take-off weight of 16,020 lb. The starboard guns were removed to make room for a pressure selector mechanism.

Since on the flight tests the port engine was set to give the correct intake ram conditions on the starboard test engine, the weight and aerodynamic condition of the aircraft were of no significance provided the required speed and altitude could be maintained. It is shown later (2.5.5) that the variation of intake efficiency with incidence was very small.

2.1.2 **Engine details.** Meteor RA.420 was fitted with two Derwent 5 engines, Nos.4044 and 4045; all Phase 1 test measurements were made on the latter engine. Prior to the tests the engines were fully calibrated by Messrs. Rolls Royce on a test bed with their flight jet pipes and single pitots. On installation in the aircraft the machined final nozzle on the test engine was replaced by one to which the rake attachments were fitted.

2.2 Instrumentation

2.2.1 **Pitot rake.** In order to reduce blockage of the final nozzle to a minimum the rake body was made as small as was consistent with stiffness (1.5/8" chord × 3/8") and was positioned 3½" behind the plane of the final nozzle, into which the 10 pitot tubes projected. Fig.2. The pitots, spaced as shown in the figure, were 1/8" O.D. 22 S.W.G. square ended tubes, sleeved over 2/3 of their length. Stainless steel was used for the tubes, and all parts of the rake and attachment brackets. The rake body was bolted to brackets on the final nozzle ring which could be attached to the jet pipe in various positions giving different diametrical positions of the rake (Fig.1). The attachement brackets were given a 5° clearance from the final nozzle to clear the jet stream. The temperature of the rake measured at maximum revs. on the ground, using therm index paint, was 500°C. The pitot tubes were brought down the body of the rake to the outside of the jet pipe, where they connected individually with copper tubing leading to a pressure selector in the starboard gun bay.

In the course of the tests an adjustable pitot tube was fitted close to the final nozzle wall so that the boundary layer thickness could be measured. This tube was connected directly to a pressure gauge in the auto observer.

The frontal area of the pitot tubes and of the rake body were 0.06 and 3 per cent of the final nozzle area respectively.

2.2.2 **Selector.** Since no space was available in the auto observer for a separate gauge for each pitot, a selector was used to relay the pressure from each tube in turn to a single pressure gauge. The selector, a Relay Box Mk.5 (Ref. No. 6K/23) was controlled by an electric timing switch which when activated selected each pitot in turn to the gauge for half a second. At the end of this period a photograph was taken automatically in the auto observer. A delay of a quarter of a second between each selection gave a total cycle time of 10 seconds. The switch was designed to complete three such cycles before shutting off; a doll's eye in the auto observer marked the beginning of each cycle.

During the initial stages of the tests a pressure gauge in the observer was permanently connected directly to tube No.1 to check that there was sufficient time for the pressure in the selector gauge to build up to give the correct pressure reading on this tube. This was verified during initial test flight, and it was assumed that the pressure in the other tubes (tubes were identical to No.1) was also being correctly recorded.

2.2.3 <u>Other instrumentation.</u>   The automatic observer contained the following instruments:

A.S.I.
Altimeter.
E.S.I. - Port and starboard engines.
Jet pipe thermometer - Port and starboard engines.
A.S.I. connected to total head ring in the starboard nacelle.   This ring had holes facing fore and aft, and neglecting velocity effects in the plenum chamber, gives a mean plenum chamber total pressure.
Differential pressure gauges connected to standard pitot and static positions in jet pipe, and to rake selector switch.
Clock.

The pilot read the air temperature by means of a balance bridge thermometer, and also the fuel flowmeter.

2.2.4 <u>Pressure gauges.</u>   The pressure gauges used for this work were differential gauges using the aircraft static as a datum.   The range of the instruments was -3 to +20 lb/sq.in.   The ranges actually covered with the pitot tubes during the tests were:

Ground run	2.3 - 10 lb/sq.in.
5,000 ft. runs	2.4 - 12 lb/sq.in.
40,000 ft. runs	1.5 - 4.3 lb/sq.in.

The accuracy and suitability of these gauges is discussed in Appendix 3.

2.3 Outline of Phase 1 tests

2.3.1 <u>General.</u>   The programme was chosen to give a comparison of the thrust estimated from the single pitot[x] and from the pitot rake readings over as wide a range of operating conditions as could be obtained subject to engine and airframe limitations.   The measurements were made with the rake in positions designated A, B, and C which are shown in relation to the final nozzle in Fig.1.

2.3.2 <u>Programme of tests</u>

<u>Ground tests.</u>   Readings were taken of the single pitot and pitot rake with the engine running at stabilised r.p.m. under static conditions when installed in the aircraft on the ground.   The aircraft was standing normally on its wheels, and the tests covered the full r.p.m. range.

<u>Flight tests.</u>   A complete set of measurements was made at each of the conditions shown in Table 1.

---

[x] Based on test bed calibration

Table 1

Altimeter	$V_i/\sqrt{p_o}$ kts.	M	$N/\sqrt{\theta_1}$
Ground run			10,000 - 14,500 by 500 intervals
5,000'	260	.394	9250 10250 11250 12250
5,000'	412	.623	11250 12250 13250 14250
40,000 or 35,000'	412	.623	11250 12250 13250 14250
40,000 or 35,000'	477	.722	13250 14250 15250 16250

It will be seen that this programme gives measurements over a common range of $N/\sqrt{\theta_1}$ at the same $V_i/\sqrt{p_o}$, at two extremes of altitude.

It was originally the intention to include a set of measurements at 25,000 feet, but these were omitted after the first rake position measurements had been made as it was evident that flying time on the calibrated engine would be running short before the programme was completed. For this reason it was also necessary to omit some of the readings at $V_i/\sqrt{p_o}$ of 260 and 477 in order to ensure a complete range at the $V_i/\sqrt{p_o}$ of 412 knots.

After completion of the programme at the first two rake positions it was found that at 40,000 feet the required indicated airspeed could not be obtained at the lower r.p.m. with the port engine at max. r.p.m. Since no engine deterioration was evident, this change in performance was ascribed to airframe deterioration. The higher altitude tests were therefore completed at 35,000 feet.

2.3.3 Flight test procedure. To complete each thrust measurement, (which involved integration of pressures at three comb positions) three runs at the same value of $V_i/\sqrt{p_o}$ and $N/\sqrt{\theta_1}$ had to be made on three flights, so that it was important for the pilot to hold steady level conditions at the selected values of $V_i/\sqrt{p_o}$ and $N/\sqrt{\theta_1}$. The pilot therefore had first to measure outside air temperature at a specified A.S.I. He then had to adjust the starboard engine r.p.m. (on which the thrust measurements were made) to give the correct value of $N/\sqrt{\theta_1}$ which he read off a card against indicated air temperatures, while controlling $V_i/\sqrt{p_o}$ at the required value by adjusting the port engine r.p.m.

When stabilised flight conditions were obtained they had to be held for some 30 seconds for the photography of three cycles of the comb pressure.

2.4 Results of Phase 1 tests. The results of the single pitot thrust calibration of the bare engine No.4045 on a Rolls Royce test bed made prior to installation in the aircraft, are given in Table 6 and the resulting effective area A_f' is plotted against H_T/P_o in Fig.3. This figure also shows the ratio

$$\frac{H_4}{H_T} = \frac{\text{Single pitot pressure}}{\text{Mean total head based on weighed thrust}}$$

The measurements made on the same engine installed in the aircraft in both ground and flight tests are given in Tables 2 to 5 where the results for each rake position are tabulated separately. All measurements are corrected for instrument error, and speeds and altitudes for pressure error. In order to assist comparison of results at different rake positions or at different altitudes, flight total pressure measurements intended to be at the same ram ratio or Mach number but actually measured at slightly different Mach numbers, are also quoted corrected to a common Mach number by the method given in Appendix 2.

Tables 2 to 5 also show calculated values of thrust but these will be discussed in para.5 since the results of Phase 2 and 3 are also concerned.

Typical distributions of total pressure across the final nozzle are shown in Fig.4. The total pressure distribution in the boundary layer in the ground runs was measured but those shown for flight conditions were derived from the ground level results at the same final nozzle Mach numbers. Total pressure distribution measurements in the boundary layer in flight could not be made due to difficulties in accurately locating the probe under prolonged conditions of vibration and heat.

Fig.5 shows non-dimensional thrusts based on rake measurements[*] plotted against $N/\sqrt{\theta_1}$ for the three rake positions and includes a later repeat run.

A comparison of single pitot pressure H_4 and mean rake total pressures $\overline{H}_5$ for ground and flight tests is shown in Fig.6. $\overline{H}_5$ was obtained by meaning rake total pressures on a momentum basis. No differentiation between the three rake positions is shown in Fig.6 because Fig.5 demonstrates that the thrust and hence the mean total head from the three rake positions are in very good agreement. To indicate the effect of total head changes on calculated thrust Fig.6 also shows the derivative $\dfrac{H}{X}\dfrac{\partial X}{\partial H}$, based on the conventional total pressure thrust relationship. (Equation 2 , Appendix 2).

Measured flight/intake air efficiencies based on readings of intake ring pressure are plotted against $N/\sqrt{\theta_1}$ in Fig.7 (at the Mach number selected for a check of the engine thrust non-dimensional relationship at 5,000 and 35,000 feet), to check that intake conditions at the two heights are not materially affected by differences in incidence and sideslip angle.

2.5 Discussion of Phase 1 results

2.5.1 Initial test bed calibration.
The effective area of the final nozzle as defined in Appendix 1 shows the normal appreciable variation with engine pressure ratio.

2.5.2 Engine deterioration check.
The single pitot measurements made at the first and last positions tested are in very good agreement and provide a check that no significant thrust deterioration took place during the Phase 1 tests, which covered the period July - December, 1950.

In addition, repeat runs for rake position B (Fig.5) are in good agreement.

2.5.3 Total pressure distribution.
The total pressure distribution at the final nozzle exit shown in Fig.4 is comparatively uniform and shows that the central wake from the conical fairing behind the turbine wheel has become fairly widely distributed. No trace could be detected at any of the rake positions of a wake from the four struts supporting the conical fairing. It is also significant that the thrusts estimated from the three rake positions (see Fig.5) were in very good agreement showing that the mean total pressure from the three pitot rake traverses must also agree closely. For this particular engine and jet pipe installation it is therefore seen that one pitot rake traverse would give an adequate sample to estimate thrust. A check for other installations would of course be necessary.

/It is..

[*] Static pressure corrections based on Phase 3 tests have been included.

It is considered that the differences in Reynolds number between ground and flight conditions would have a small effect on the boundary layer and any small inaccuracy in the flight boundary layer derived from ground test results, would have a negligible effect on flight thrusts estimated from the rake.

2.5.4 Comparison of single pitot and mean rake total pressures. The results shown in Fig.6 indicate that there is some change in the ratio $\frac{H_4}{H_5}$ with change in test conditions. Thus $\frac{H_4}{H_5}$ at the higher pressure ratios is significantly higher both under ground installed conditions and at 35,000 feet than at 5,000 feet. These differences due to changes in total pressure sampled by the single pitot are equivalent to changes of thrust of the order of 3%. The relationship between the measured points and the derived test bed curve of Fig.6 will be discussed in para.5.

2.5.5 Air intake efficiencies. Fig.7 shows that air intake efficiencies at M = .62 at 5,000 and 35,000 ft. do not differ by more than 2% which would be equivalent to an increase in thrust at the higher altitude of the order of $\frac{1}{2}$% under these conditions. Thus the comparison of thrust at the two heights required for a check on the non-dimensional relationship will not be vitiated due to the effects of incidence and sideslip on air intake efficiency.

3. Phase 2 tests. Test bed measurements on bare engine with pitot rake

3.1 General. In order to check the validity of the rake thrust as being an absolute measure of thrust it was required to compare test bed thrustmeter readings with the thrust derived simultaneously from the rake total pressure measurements. It was also required to check that the presence of the rake was not affecting the engine operating conditions through blockage of the final nozzle. Tests to this programme were made by Rolls Royce whose help in this matter is acknowledged.

Tests were made on a Derwent 5 engine which was run on the test bed, with rake fitted and rake removed, under otherwise identical conditions.

3.2 Description of test bed and instrumentation. The tests were made on a Rolls Royce Sinfin production type test bed which was equipped with a detuner silencer and a thrustmeter of the weighing type. The engine used for the tests was Derwent 5 No.3381.

The rake, single pitot and final nozzle static pressures were measured on mercury manometers. Normal test bed instrumentation was used for other engine measurements, the engine r.p.m. being set with a stroboscope.

Static pressure measurements were made near the exit of the final nozzle on four wall statics fitted at 90° stations; these consisted of $\frac{1}{8}$" O.D. steel tubes brazed into holes in the final nozzle ring, the tubes being machined flush with the inside of the nozzle. They were located as shown in Fig.1. The rake was otherwise as detailed in 2.2.1. (Phase 1).

3.3 Tests carried out

The following tests were made:

(i) Full rating run with flight nozzle and rake fitted
(ii) "   "   "   "   "   "   "   " removed.

In each case full engine measurements of thrust, r.p.m. temperatures and pressures were made, and in (i) rake total head measurements were taken.

3.4 Results of Phase 2 tests

The relevant results are given in Tables 7 and 8. In Fig.8 the thrustmeter measurements for runs (i) and (ii) and the thrusts X_G derived by the conventional total pressure-thrust relationship, Equation 2 Appendix 2, from the rake total pressures in run (ii), are illustrated.

Fig.9 shows the jet pipe temperatures and the single pitot total pressure values for the two runs.

The mean difference between test bed thrustmeter measurements X_m and those derived from the rake total pressure values X_G, measured simultaneously, is 6% above 11,000 r.p.m. Table 8.

3.5 Discussion. Part of the difference between X_m and X_G of 6% can be attributed to the drag of the rake which is included in the thrustmeter measurements.

Rake drag = difference between X_m, rake on and off,
plus rake interference on thrust.

The difference between X_m rake on and off taken from Fig.8 is 2%. The interference of the rake can be estimated from the single pitot readings rake on and rake off. Fig.9. The change is small and is not much greater than the accuracy of measurement. However the change is significant and amounts to about ½ per cent increase in thrust due to the presence of the rake at higher r.p.m. This increase is confirmed by a very small increase in jet pipe temperature between the two runs.

Thus the rake drag will be $2\frac{1}{2}$%, giving a drag of 90 lb./choke at I.C.A.N. ground conditions. This is a reasonable figure for a body of these dimensions and chord thickness ratio of 4.3.

Since the rake would be expected to give (thrustmeter reading + rake drag), the discrepancy between actual and expected rake thrust is $3\frac{1}{2}$ per cent.

This discrepancy has been verified by repeat tests on another Derwent engine, and a discrepancy of the same order observed on an axial type engine (unpublished data).

An investigation indicated that the static pressures at the final nozzle might differ sufficiently from the assumed theoretical values to cause this discrepancy, and Phase 3 tests to measure these static pressures were therefore put in hand.

4. Phase 3 tests. Final nozzle exit static pressure measurements on engine installed in aircraft

4.1 Introduction. In the Phase 1 tests only final nozzle exit total pressure measurements were made on the assumption that the final nozzle static pressure was uniform and equal to the theoretical value. Phase 2 tests showed that there was a discrepancy between the pitot rake thrust derived on this basis and the balance thrust, which was ascribed to this assumption regarding static pressure being incorrect.

It was therefore decided to make measurements of the final nozzle static pressure under the same ground and flight conditions used in Phase 1, to check the magnitude of this effect and to enable a thrust correction for the actual static pressures to be derived.

At this stage it was not possible to make the static measurements on the same engine or aircraft as neither were available. The original flight final nozzle complete with rake was therefore fitted to another Meteor 4, and some checks on engine to engine final nozzle static pressure variation were also obtained.

For the ground and flight measurements of static pressure the static sources used were a static head fitted in place of the centre pitot on the rake and two wall statics. Measurements were initially made only at the centre and walls since it was thought that any swirl in the jet would adversely affect the accuracy of a static head at any other position, and in any case an appreciable departure from the theoretical static pressure was not expected.

/The rake..

The rake centre static was calibrated against static pressure measurements made at the wall of a long tube suspended along the jet pipe axis during a ground run.

When the initial ground and flight tests had been completed it was found that there was a considerable difference in the static pressure at the centre and the wall of the final nozzle, and that it would be necessary to know the approximate static pressure distribution between these points to establish the required correction. The rake was therefore modified by the replacement of two more pitots by static heads, at convenient radii, and a final ground run made to measure the static pressure at these points.

It was appreciated that the accuracy of these latter static heads was likely to be affected by any swirl in the jet flow, but great accuracy was not required since the exact distribution of static pressure had a small effect on the correction. No figures of the swirl likely to be encountered were available.

4.2 Description of instruments

4.2.1 Long tube for calibrating rake central static. In order to measure under ground running conditions the true static pressure at the centre of the final nozzle, for calibration of the rake centre static, a long tube was suspended along the axis of the jet pipe. It was suspended between the centre of the turbine exhaust cone and a support downstream of the final nozzle (see Fig.1). The tube was stainless steel of $\frac{1}{2}$" O.D. and was 102 inches long. The upstream end was sealed, and was welded into a hole at the apex of the turbine cone. The downstream end ran through a sleeve in a streamlined stainless steel strut which was bracketed to the final nozzle. A compression spring between the downstream edge of the strut and a washer pinned to the end of the tube kept the tube in tension. The strut was $1\frac{1}{2}$ inches thick, having a $3\frac{1}{4}$ inch chord. The leading edge of the strut was located 15 x strut thickness downstream of the two 1/16" D static holes drilled in the tube at the plane of the final nozzle. This distance, $22\frac{1}{2}$ inches, was chosen as giving negligible interference at the static holes upstream (Ref. 5).

A differential pressure gauge was connected to the tube which, apart from the static holes, was sealed.

The compression spring was found to lose its temper during the ground running but the tube was sufficiently stiff to remain stable and without vibration except for a period between 12,000 and 13,000 r.p.m.

The tube was a unit with its turbine exhaust cone and in order to fit or remove this unit the engine had to be removed from the airframe.

4.2.2 Rake static. The static heads fitted to the rake were 3/16" in diameter and had a hemispherical head. The distance from the two 1/16" diameter static holes to the head was five tube diameters. Fig.2.

The two wall statics used were as described in para.3.2, and were on a diameter at right angles to the rake diameter.

The initial calibration and flight measurements were made on the wall and central statics; for the final ground run two additional statics were added to the rake at radii of 4 and 6 inches. The same correction factor was used for these heads as was derived for the centre static head.

All static pressure measurements were made on differential pressure gauges (-3 to +20 lb/sq.in.).

4.3 Outline of tests

4.3.1 General. The aircraft used for these tests was Meteor RA.438; the condition of the aircraft was not relevant to the tests.

/The engine..

The engine used for the calibration of the single pitot against the long tube was Derwent 5 No.4166. The ground and flight pressure measurements were made on Derwent 8 No.4905. The Mark 8 differs mainly from the Mark 5 in the material of the rotating guide vanes. Other differences are external and there is no relevant change of nominal thrust or internal geometry.

4.3.2 **Calibration of rake centre static.** With the long tube fitted a ground run was made through the maximum r.p.m. range obtainable. Readings of static pressure were taken on a differential pressure gauge connected to the long tube.

To reach as high a Mach number as possible in the final nozzle a concession to operate up to 15,250 r.p.m. had been obtained, subject to temperature limitations, but 14,900 were the maximum achieved.

With the long tube removed and the rake fitted, the ground run was repeated, through the same r.p.m. range. The static pressure at the centre static was recorded on a differential pressure gauge.

4.3.3 **Flight measurement of final nozzle static pressures.** The static pressure at the wall and centre of the final nozzle and the single pitot total head reading were recorded at each of the flight conditions given in Table 1.

4.3.4 **Ground measurement of final nozzle static pressures.** On completion of the flight tests the rake was modified by the addition of two more static heads as described in para.4.2.2.

A ground run was then carried out and the pressures at the two wall statics and three static heads were recorded. The pressures at the single pitot and the remaining rake total head tubes were also measured.

4.4 **Results of Phase 3 tests**

4.4.1 **Ground installed static pressure measurements.** The static pressures measured at the centre of the final nozzle by the long tube and the rake centre static are shown in Fig.10. The correction factor for the static head on the rake derived from these results is given in Fig.11 which also includes a correction estimated from Ref. 5.

Measurements at the centre static after the flight programme had been completed, using a different engine, are also shown on Fig.10.

The static pressure distribution across the final nozzle on the final ground run is plotted in Fig.12. Included in this figure are similar unpublished measurements made by N.G.T.E.

4.4.2 **Flight static pressure measurements.** The corrected static pressure in the final nozzle expressed as a ratio of the mean dynamic head is given for the full flight programme in Fig.13. Wall static measurements made on the test bed are also included. The wall readings given are the mean of two wall statics, which were in reasonably close agreement.

The method of correcting thrust estimated from pitot rake readings due to departures in final nozzle static pressure from the conventionally assumed values is given in Appendix 2. In the one dimensional case, it consists of a factor A_6/A_5 which is a function of the final nozzle static pressure. This factor has been plotted for a range of nozzle exit static pressures, and the results are given in Fig.14.

The flight and ground results were estimated using Fig.14 and the measured wall and centre static pressures of Fig.13 weighted in accordance with the static pressure distribution of Fig.12. The resulting corrections are shown in Fig.15.

4.5 Discussion of Phase 3 tests

4.5.1 Calibration of central static. The accuracy of the calibration of the central static on the rake depends on whether vibration of the static tubes could be affecting the static pressure readings and on whether the presence of either the long tube or the pitot static rake affects the final nozzle static pressure.

Concerning the effects of vibration, the static pressures using the long tube as a source appear consistent. The tube remained steady over the engine speed range except for a period between 12,000 and 13,000 r.p.m., when a lateral vibration of about $\frac{1}{2}$ an inch developed. The pressure recorded did not appear to be in any way affected by this vibration and remained consistent.

The rake blockage effects were found to be very small in the Phase 2 tests, while the central tube blockage will be smaller still, so with the relatively small rate of change of P_5 with $N/\sqrt{\theta_1}$ (Fig.10) or H_5/p_0 (Fig.13) calibration errors due to blockage can be considered unimportant for the accuracy required in the present tests.

The correction factor for the static head (Fig.11) unfortunately does not extend to very high values of local Mach number, or $\bar{H}_5/P_5$, although the maximum possible r.p.m. was used on the ground runs. This is due to the fact that when $\bar{H}_5/p_0$ approaches the choking value, the high static pressure at the centre of the jet means that the Mach number there is still low. Over the range of tests the correction factor agrees to 1% of the dynamic head with the factors for similar static tubes described in Ref.5. (See Fig.11).

4.5.2 Discussion of flight and ground measured static pressures. The results plotted in Fig.13 show that the centre static pressures are remarkably high, particularly in flight, and to a less extent in static ground tests. The wall static pressures agree closely with conventional theoretical values above the choke, but are naturally influenced more by changes in flight conditions when below the choke. It will be noted that there are appreciable changes between static pressures in flight and on the ground below the choke.

Another result of importance to this report is that the central statics measured on two different engines and shown plotted in Fig.10 are in very close agreement which confirms the view from general considerations that engine to engine final nozzle static pressures at given pressure ratios would be expected to agree substantially.

The static pressure distribution across the final nozzle measured on the ground runs is fairly independent of jet Mach number, and agrees reasonably with the N.G.T.E. unpublished results, also shown in Fig.12. These latter measurements were made with an N.P.L. pitot static head in a Derwent 5 flight final nozzle under test bed conditions. The values very near the wall are likely to be incorrect due to interference and have not been shown.

The additional static tubes not at the jet centre may have been affected by any swirl present in the jet flow. No information as to the likely magnitude of this swirl has been obtained, but it seems unlikely that it would be greater than 2 or 3° which would have a small effect on the static readings.

4.5.3 Corrections to Phase 1 rake thrusts. The required corrections to the thrusts derived from rake total pressure measurements assuming the theoretical static pressures in the final nozzle are given in Fig.15.

The correction increases with flight Mach number and decreases with increase in total pressure. Thus at maximum level speeds the correction is small, about $\frac{1}{2}$% in gross thrust.

At cruising conditions the correction is larger, of the order of 2%, and at conditions such as would be encountered in a decelerated level, amounts to about 6%.

5.   Consideration of combined tests

The individual results of Phase 1, 2 and 3 tests have been considered in detail in paragraphs 2, 3 and 4.   To compare thrusts under flight conditions estimated from single pitot with fully corrected thrusts estimated from pitot static rake measurements, the results of Phase 1, 2 and 3 must however be considered in conjunction.   It is therefore proposed/summarise the individual results which will be used, outline the method of combining results, and finally to present and discuss the results of the combined tests.

5.1   Summary of individual results

5.1.1   Phase 1 tests.   Measurement in flight and on the ground of single pitot and pitot rake total pressures on Derwent 5, No.4045 in Meteor 4 RA.420.   The tests covered a range of conditions as wide as possible, which are summarised in Table 1 on page 8.

These tests measured the ratio $H_4/\bar{H}_5$ = $\dfrac{\text{single pitot total pressure}}{\text{mean rake total pressure}}$, which may be considered as the single pitot "sampling factor" of the jet final nozzle total pressure, and established that its magnitude has small but significant changes at given engine conditions between ground and flight tests and between flight tests at high and low altitudes which would affect the single pitot method of estimating flight thrusts. (Fig.6).   The tests also demonstrated

(1)   That any troughs in the final nozzle total head distribution due to strut wakes did not have any serious effects, as the mean total pressures at three rake positions were in good agreement (Fig.5).

(2)   No significant engine deterioration occurred during Phase 1 tests (Fig.5).

(3)   The air intake efficiency in flight at a given Mach number (or ram ratio) was not appreciably affected by altitude or sideslip effects.   (Fig.7).

(4)   The scatter in $H_4/\bar{H}_5$ of single observations is of the order of $\pm1\%$ except in flight at high altitudes when it increases to ±2 to 3% (See Appendix 3).

5.1.2   Phase 2 tests.   Measurements made at the request of A.& A.E.E. by Rolls Royce on a test bed to compare thrust measured by balance, and estimated from pitot comb.   The engine was Derwent 5 No.3381 which was fitted with the same final nozzle as was used in the Phase 1 tests.

These tests demonstrated that the drag of the rake was of the order expected and that due to the presence of the rake the engine thrust was increased by $\frac{1}{2}\%$ or only just significantly.   (Fig.8 and 9).   The main result was that the thrust estimated directly from pitot rake readings assuming jet exit static pressure equal to atmospheric was $3\frac{1}{2}\%$ higher than the test bed balance thrust.

5.1.3   Phase 3 tests.   Measurements of static pressure at the jet final nozzle exit on the ground and in flight.   The measurements were made on Derwent 8 No.4905 fitted with the same final nozzle as was used in Phase 1 and 2 tests, and was installed in Meteor 4 RA.438.   These tests included a calibration of static tube fitted to the rake at the jet centre, flight and ground measurements of wall and centre static pressures and measurement, on the ground, of the static pressure distribution across the jet exit.

The main results were:-

(1)   The measured calibration of the central static was satisfactory and agreed to 1% of the dynamic head with other published work. (Figs.10 and 11 and Ref.10).   Extrapolation to higher final nozzle Mach numbers obtained in flight was necessary.

/(2)..

(2) Static pressures in flight and on the ground differed markedly from atmospheric when the jet was not choked, the centre static being 30% of the dynamic head above ambient atmospheric in some cases. Above the choke wall statics agreed with the theoretical choked values but the centre statics were again appreciably higher. (Fig.13).

(3) The measured static pressure distribution across the jet exit was not markedly affected by jet pressure ratio and agreed with some other unpublished measurements by N.G.T.E. (Fig.12).

These results showed that a pitot rake is inadequate to give an absolute measure of thrust and must be backed by static measurements. Corrections for measured static pressure to thrust estimated direct from pitot readings only (see Appendix 1) are given in Fig.14. The results also showed a change of static pressure between static and flight conditions which would affect the single pitot method of estimating thrust.

5.2 **Method of combining results to obtain fully corrected thrusts for pitot static rake.** It is now clear that to obtain fully corrected thrust directly by the momentum method it is necessary to make measurements with a pitot static rake. In fact, the pitot rake readings were obtained on one engine and the static measurements were made on another nominally identical engine with the same final nozzle, and thrusts from the pitot rake results obtained can only be corrected for static pressure on the assumption that variations in the magnitude and distribution of static pressure between nominally identical engines is insignificant. Ground static pressure measurements at the jet centre on two engines shown in Fig.10 are in very close agreement, while equally close agreement has been obtained on wall statics measured on ground tests on two other engines. Hence, bearing in mind that appreciable changes of static pressure are required to effect the thrust significantly[x] the above assumption is considered justified at any rate for the particular installation.

Further, the static pressure distribution was measured on the ground, so it is necessary to assume that the distribution is similar in flight. Since wall and centre values are available in flight the error introduced on this account must be very small indeed.

With these assumptions on static pressure, corrections to be applied to the pitot rake measurements to give fully corrected rake thrust have been estimated from the flight static pressure measurements by the method of Appendix 2 and are shown in Fig.15.

As stated in paragraph 5.1.2, thrusts estimated directly from pitot rake readings assuming exit static pressures equal to atmospheric were $3\frac{1}{2}\%$ higher than test bed balance thrusts measured simultaneously. Only wall static measurements were made on the test bed, but these are of the same order as wall statics on ground tests (see Fig.13). Under the latter conditions the static pressure correction would reduce the $3\frac{1}{2}\%$ discrepancy to 2%. Whether this 2% discrepancy is the sum of various errors in the measurements including windage in the test bed, or is due to some more fundamental difference, has not been established. The assumption has been made in presenting thrusts calculated from combined pitot static readings that they are basically correct, and no 2% reduction has been applied. Such thrusts will be nominated X_R.

5.3 **Thrusts estimated from combined results.** Values of X_R estimated on the basis of paragraph 5.2 are included in Tables 2 - 5, and have been used to estimate single pitot effective areas A_p',

/(defined..

$\frac{\Delta P}{H-P}$ = 0.10 gives 2% change of thrust at $\bar{H}/P_0$ = 1.4
and 1% change of thrust at $\bar{H}/P_0$ = 1.8

(defined by $A_f' = \dfrac{X_R}{\text{thrust per unit area given by single pitot}} = \dfrac{X_R}{X_{GP}}$)

which are plotted in Fig.16 against $\bar{H}_5/P_o$ and in Fig.17 against $N/\sqrt{\theta_1}$. The test bed calibration for this single pitot-jet pipe combination is reproduced from Fig.3 for comparison with these results. It is usual practice in using a single pitot in conjunction with a test bed calibration to assume the effective area to remain constant above the highest pressure ratios reached on the test bed. This extrapolation is shown on Fig.16. Values of the effective area at high total pressures for a Derwent 5 engine derived from measurements made in the Munich altitude test chamber, Ref.6, are included in this figure.

It may be noted that % change in A_f' between calibration and test condition by definition equals % error in thrust by the single pitot method.

The conventional non-dimensional relationship for jet thrust is that

$$\frac{X_R}{P_o} = f_1 \left(\frac{N}{\sqrt{\theta_1}} , \eta_i, M \right) \quad \text{or} \quad f_2\left(\frac{N}{\sqrt{\theta}} \cdot \frac{P_1}{P_o} \right) \quad \text{which however neglects changes}$$

of Reynolds number and combustion efficiency with altitude. To check this relationship measurements of X_R made at $M = 0.62$ at 5,000 and 35,000 ft. have been plotted against $N/\sqrt{\theta_1}$ in Fig.18. It has been demonstrated in para. 2.5.5. that η_i is independent of altitude at fixed M so that X_R/P_o for the two heights can be compared directly. Values of X_{GP}/P_o are also plotted in Fig.18.

In Fig.19, measurements of X_R made at 5,000 and 35,000 feet, but at several Mach numbers, are plotted in the form

$$\frac{\dfrac{X_R}{A_f' P_o} + 1}{R_{01}} \quad , \quad \text{against } N/\sqrt{\theta_1} \text{ in which form they are theoretically}$$

independent of ram ratio above the choke. The derivation of this parameter is explained in Appendix 4. Also plotted in this figure are the test bed (balance) thrusts, calculated taking $R_{01} = 1.0$, and the non dimensional performance graphs for the Derwent 5 engine taken from the Rolls Royce brochure (Ref.10).

The experimental error in the measurement of X_R and X_{GP} is discussed in Appendix 3.

5.4 Discussion of combined results

5.4.1 Errors in flight thrust estimated from single pitot with a test bed calibration.
All single pitot effective areas in the ground run and flight cases in Fig.16 are lower than the test bed effective areas (except at very low total pressure ratios of about 1.2). This shows that if the test bed effective area is used under these conditions the thrust would be over-estimated. In general there appears to be a steady rise in the actual effective areas under flight conditions between total pressure ratios of 1.7 and 2.6, the highest value reached on the tests. This rise brings the actual effective areas into better agreement with the extrapolated test bed values at the highest total pressures reached at 35,000 feet.

In general there appears to be little Mach No. effect in the values of A_f' at the same altitude.

At a Mach number of 0.39 at 5,000 feet there is approximate agreement between the test bed and flight values over the range of total pressures covered in the tests and there is little difference between the effective areas at this Mach number and the results at a Mach number of 0.62 at 5,000 feet, where they can be compared over a common range of $\bar{H}_5/P_o$. At this higher Mach number the difference between test bed and flight values increases to 4% at $\bar{H}_5/P_o$ of 1.6, and then decreases at higher $\bar{H}_5/P_o$, being about $2\frac{1}{2}\%$ at $\bar{H}_5/P_o$ of 1.75.

/At a..

At a Mach number of 0.62 at 35,000 feet the error involved in the use of the test bed effective areas is largest and is of the order of 5 - 6% at $\bar{H}_5/P_0$ values between 1.5 and 1.7. Again the steady increase of effective area with increasing total pressure brings flight values into closer agreement with the extrapolated test bed curve. The difference is small at $\bar{H}_5/P_0$ values of 2.5. The values of effective area at a Mach number of 0.72 at 35,000 feet are in general agreement with those at M = 0.62. The difference between the flight values and the extrapolated test bed curve decreasing from 4 to 2% approximately over the $\bar{H}_5/P_0$ range of 1.9 to 2.5.

Measurements made in the installed ground case show that the single pitot effective area under these conditions is in approximate agreement with the test bed calibration at values of total pressure of 1.2, but that as $\bar{H}_5/P_0$ is increased a discrepancy, amounting to 3% at $\bar{H}_5/P_0$ = 1.3 and 5% at $\bar{H}_5/P_0$ = 1.55, is encountered. This difference between the ground installed calibration of the single pitot using a pitot static rake and the test bed thrustmeter calibration is dealt with below when the implications of using such a rake calibration for flight measurements are discussed.

The 2% difference between test bed balance and rake thrust measurements, would, if applicable in the ground installed and flight cases, increase the percentage differences detailed above by 2%.

The individual contribution to the error in single pitot thrust of changes in H_4/H_5 and changes in static pressure between calibration and test conditions can be examined in Figs.6 and 15. Above the choke the larger part of the error is contributed by changes in H_4/H_5. At lower pressure ratios it is more difficult to generalise but both effects are appreciable.

5.4.2 <u>Errors in flight thrust estimated from single pitot used in conjunction with ground installed calibration against rake thrust X_R</u>. Again referring to Fig.16, the errors in thrust measured in flight by the single pitot method used in conjunction with a ground installed calibration against rake thrust X_R will in general be less than those involved when the test bed calibration is used. This is fortuitous, and is accounted for by the fact that under ground installed conditions the single pitot samples a total pressure corresponding more closely with those sampled in flight than on the test bed. (Fig.6).

Over the total pressure range covered on the ground run, agreement between the single pitot ground calibration and the flight values is within 1 or 2 per cent.

If the ground calibration is extrapolated above the highest pressure ratios obtained assuming A_f' to remain constant, the single pitot thrusts would be sensibly correct at a pressure ratio of 1.6. With increasing pressure ratios the single pitot thrust would become progressively low, and would be about 3% low at H_5/P_0 = 2.5.

In this case the 2% difference between test bed balance and rake thrust measurements, if applicable equally to ground and flight conditions, would not alter the figures quoted above.

5.4.3 <u>Choice of abscissa for plot of A_f'</u> The single pitot effective area A_f' calculated on rake or test bed thrust can be plotted against H_5/P_0 or $N/\sqrt{\theta_1}$. It has been usually considered that H_5/P_0* is the more logical parameter. This is confirmed in Figs. 16 and 17, where the spread of A_f' at any engine condition specified by H_5/P_0 is less than the spread at a condition similarly specified by $N/\sqrt{\theta_1}$. It is therefore not proposed to discuss Fig.17.

5.4.4 <u>Check on non-dimensional thrust relationship</u>. Examination of Fig.18 shows that at lower r.p.m. there is good agreement between the rake thrust values X_R/P_0 at 5,000 and 35,000 feet, but with increasing r.p.m. the higher altitude thrusts fall progressively below those for 5,000 feet. The fall off in gross thrust at 35,000 feet compared with that which would be predicted from the 5,000 feet results according to the non dimensional theory amounts to 7% at the maximum r.p.m. reached in the tests.

*Or H_4/P_0

/The single..

The single pitot thrust X_{GP}/P_0 calculated using the test bed effective area also demonstrates this effect, but less clearly, since the effective areas used are in error and mask the effect.

Fig.19 which includes additional results at M = .39 and .72 again demonstrates the fall in non-dimensional thrust with altitude. Comparing measured and brochure figures, shows that the brochure figures tend to be optimistic at high altitude and pessimistic at low altitude. The engine test bed thrusts are in good agreement with the curve at a ram ratio of 1.0.

This fall off of X_R/P_0 at high altitude which is ascribed to changes in Reynolds number or combustion efficiency has been previously noted in Refs.7 and 8.

6. Conclusions

The tests have demonstrated that the assumptions inherent in the single pitot method of estimating gross thrust based on a calibration of the engine on a test bed are not quite accurate. Thus changes in total pressure distribution between test bed and flight conditions result in single pitot sampling errors of up to 3% in total head, equivalent to some 5% in thrust. Again changes in the magnitude of the static pressure at the jet exit between test bed and flight conditions are quite large, and would result in thrust changes of up to 3%. These two effects are additive but were measured on different engines. There are, however, good grounds to conclude that the single pitot method based on a test bed calibration could give a thrust error of up to 6%. Comparative measurements on a test bed showed the thrust from pitot static rake readings to be 2% higher than thrust measured by the test bed balance. Further investigation would be needed to determine the cause of this discrepancy, but the implication is that total single pitot errors quoted above may be increased by the order of 2%. A further assumption of the single pitot method, that above the highest final nozzle pressure ratio reached on the test bed the single pitot effective area remains constant, is also not quite accurate; in fact it increases slowly.

From the above conclusions it follows that to make absolute measurements of thrust by the momentum method, it will be necessary to use a pitot static rake. Such measurements of total and static pressure on a Derwent 5 in a Meteor 4 on the ground gave a calibration of the single pitot at least as good, if not better, than the test bed calibration.

Using the pitot static rake as an absolute measure of thrust, it has been possible to check the effect of altitude on the generally accepted non-dimensional relationship for the thrust of jet engines, and the conclusion reached is that there is a fall off in non-dimensional thrust at 35,000 ft. compared with 5,000 ft. of the order of 7%.

Other detailed conclusions are:-

(1) Differential pressure gauges of different ranges for high and low altitude pressure measurements are needed to obtain good accuracy at high altitude.

(2) An adequate calibration of static tubes can be estimated from the literature if care is taken.

(3) The development of an integrating rake would be advantageous for use if further flight rake measurements are to be made.

7. Further developments

It is suggested that to confirm the findings of the present report, and to provide information on other engine types, test bed, ground and flight tests with a pitot static rake fitted should be made on another engine type, preferably with an axial compressor. The use of an integrating rake should be investigated.

/List of symbols..

X	Gross thrust
X_T	Engine gross thrust measured on test bed balance
X_G'	Ground or flight gross thrust derived from pitot rake total pressure measurements, corrected for boundary layer and using hot area of final nozzle
X_G	X_G' corrected to nominal $V_i/\sqrt{P_o}$
X_R	X_G corrected for static pressure in final nozzle
X_{GP}	Ground or flight gross thrust measured by standard jet pipe single pitot, using test bed effective area correction based on H_4/P_o, corrected to nominal $V_i/\sqrt{P_o}$
x_{GP}	Thrust per unit area based on single pitot total pressure
x'	Momentum thrust per unit area – at actual $V_i/\sqrt{P_o}$
x	Momentum thrust per unit area – corrected to nominal $V_i/\sqrt{P_o}$
P	Static pressure
P'	Static pressure measured by rake static head before correction
P_o	Ratio of static pressure to selected standard $= P_o/14.7$
H'	Total pressure at actual $V_i/\sqrt{P_o}$
H	Total pressure corrected to nominal $V_i/\sqrt{P_o}$
$\bar{H}$	Mean total pressure across final nozzle area (hot), meaned from rake measurements on a momentum basis
$\bar{H}_T$	Mean total pressure across final nozzle area (hot) based on weighed thrust
t	Temperature $^{\circ}C$
T	Temperature $^{\circ}K$
T_1	Total temperature at engine intake $= T_o + v^2/2Kp$
θ	Ratio of T to selected standard $= T/288$
θ_1	Ratio of T_1 to selected standard $= T_1/288$
Kp	Specific heat at constant pressure
M	Gas flow, lb/sec.
ζ	Density
γ	Ratio of specific heats $Kp/Kv = 4/3$ for jet gases
J	Mechanical equivalent of heat
R	Gas constant
N	Engine r.p.m.
A_f	Final nozzle area – cold
A_f'	Effective final nozzle area for single pitot $= \dfrac{\text{Thrust by rake or test bed balance}}{\text{Thrust per unit area given by single pitot}} = \dfrac{X_R}{x_{GP}} \text{ or } \dfrac{X_T}{x_{GP}}$
η_1	Intake efficiency $= \dfrac{H_1 - P_o}{H_o - P_o}$
R_{01}	Ram ratio P_1/P_o
C_p	Rake static correction factor $= \dfrac{P_{5G} - P_{5C}'}{\bar{H}_5 - P_{5C}'}$
h_p	Pressure height, feet
V_i	Equivalent air speed, knots
v	True airspeed, ft/sec.

Subscripts

o	Refers to free stream conditions
1	Refers to conditions in nacelle at entry to compressor
4	Refers to conditions in jet pipe at standard single pitot position
5	Refers to conditions at final nozzle
C	Refers to centre of final nozzle

References

Ref. No.	Author	Title, etc.
1	-	Measurement of thrust of Jet Engines in Flight. AAEE/5781/g7/KJL.
2	D. R. Andrews	Some considerations of jet thrust measurements in flight, with particular reference to the trunnion thrust method. R.A.E. Technical Memorandum No. Aero 292. A.R.C. 15,265.
3	D. J. Higton and R. H. Plascott.	Measurement of overall drag of an aircraft at high Mach numbers. R. & M. 2748. January, 1949.
4	Bengt Jakobsson	Definition and measurement of jet engine thrust. Journal of the Royal Aeronautical Society. April 1951.
5	L. N. Krause.	Effects of pressure rake design parameters on static-pressure measurements for rakes used in subsonic free jets. N.A.C.A. Tech. Note 2520.
6	-	The testing of the Derwent Series V engine No. 3152 in the high altitude test chamber at Munich. Rolls Royce Report SGH/GF.1/AM. 5/6/46.
7	Barson & Wilsted.	Altitude chamber performance of British Rolls Royce Nene 2. engine. I Standard 18.75 inch diameter jet nozzle. N.A.C.A. RME.9123. TIB.2121.
8	Armstrong, Wilsted and Vincent.	Altitude chamber performance of British Rolls Royce Nene 2 engine II 18.41 inch diameter jet nozzle. N.A.C.A. RME.9127, N.A.C.A. TIB.2133.
9	-	Total pressure and temperature traverses on Nene No. 193. Rolls Royce Report Dor/GDM/ TM4/RMW. 19.1.51.
10	-	Derwent Marks 5, 8 and 501 engines. Established Performance data and installation notes. T.S.D. Publication 238, June 1949. Amended June, 1951.
11	A. D. Young	Note on a method of measuring profile drag by means of an integrating comb. R. & M. 2257. May, 1939.

Theory of thrust estimation from momentum measurement

1. The thrust of a jet engine is normally defined as the change in momentum of the internal flow. The planes before and behind the engine between which the momentum change is measured must then properly be taken as those where the static pressure of the internal flow is equal to the ambient static pressure
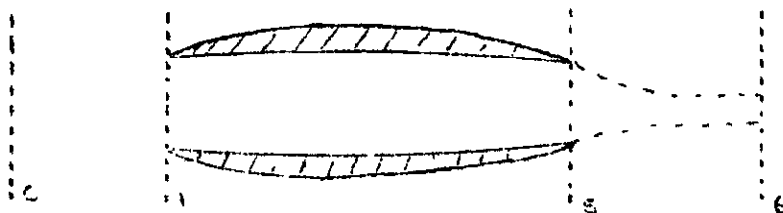
The nett thrust is then

$$X_N = -\frac{M_o V_o}{g} + \frac{M_6 V_6}{g} \qquad \dots\dots\dots(1)$$

where M is the internal engine mass flow, the plane 0 is at infinity and V_o is the flight speed, and the plane 6 is such that $P_6 = P_o$.

For a supersonic jet, plane 6 may be taken at the throat (Ref.4) and (1) becomes

$$X_N = -\frac{M_o V_o}{g} + \frac{M_6 V_6}{g} + (P_6 - P_o) A_6 \qquad \dots\dots\dots(1a)$$

$$\text{where} \quad P_6 = \frac{H_6}{\left(\frac{1 + \gamma}{2}\right)^{\frac{\gamma}{\gamma - 1}}}$$

2. In the static case $V_o = 0$ and the nett thrust is equal to the gross thrust,

$$X = \frac{M_6 V_6}{g} + (P_6 - P_o) A_6 \qquad \dots\dots\dots(2)$$

where the pressure term is zero below the choke.

This is the thrust which is measured on the test bed, subject to minor effects of windage over the engine exterior from induced flow which should be negligible in a properly designed test bed.

If it is assumed that the static pressure in the plane of the final nozzle, P_5, is equal to P_o below the choke and to $H_5 / \left(\frac{\gamma + 1}{2}\right)^{\frac{\gamma}{\gamma - 1}}$

above the choke, the plane 6 is then at the final nozzle, 5, and

$$X = \frac{M_5 V_5}{g} + (P_5 - P_o) A_5 \qquad \dots\dots\dots(3)$$

the pressure term being zero below the choke.

This may be shown to give (as in ref.3)

$$\frac{X}{A_5 P_o} = \frac{2 J K_p}{R} \frac{H_5}{P_o} \left[\left(\frac{H_5}{P_5}\right)^{\frac{1}{\gamma}} - \frac{P_5}{H_5} \right] + \left(\frac{P_5}{P_o} - 1\right) \qquad \dots\dots\dots(4)$$

from which $\frac{X}{P_o}$ is obtained as a function of $\frac{H_5}{P_o}$ only, using the assumed values of P_5.

If the distribution of H_5 is non-uniform over the final nozzle $\frac{X}{P_o}$ may be obtained by integrating (4) over the nozzle area.

3. Generally, however, $P_5 - P_0$ is found to have higher values than those assumed. The effect of this will be for the jet stream to contract further from 5 to 6 where the assumed pressure is reached and there will be a vena contracta at 6.

The thrust which will be measured on the thrustmeter is given by equation (2) and this will differ slightly from that derived from equation (3) by an amount arising from the pressure at the jet stream boundary between 5 and 6.

Thus
$$\frac{M_5 V_5}{g} + (P_5 - P_0) A_5 = \frac{M_6 V_6}{g} + (P_6 - P_0) A_6 + \int_5^6 P dA \quad \dots\dots(5)$$

The term $\int_5^6 P \, dA$ will be associated with an equal external drag at the rear of the engine.

4. In flight it is not practical to make measurements in plane 6 as downstream of the jet exit the internal and external flows mix and it will not be possible to measure the momentum of the internal flow.

The gross thrust X_R may however be derived from a pitot-static traverse in the final nozzle on the assumption of isentropic expansion with no mixing losses between 5 and 6 and this is the basis of estimation of gross thrusts calculated from pitot static measurements used in the present report.

X_R has been derived by first obtaining X_G as the thrust value given by equation (4) with the usual assumptions as to static pressure. This is equivalent to obtaining

$$X_G = \frac{\rho_6 A_5 V_6^2}{g} + (P_6 - P_0) A_5 \quad \dots\dots\dots(6)$$

since the total and static pressures used are really those corresponding to plane 6 ($H_5 = H_6$).

The true gross thrust is, from (2) in this Appendix

$$X = \frac{\rho_6 A_6 V_6^2}{g} + (P_6 - P_0) A_6 \quad \dots\dots\dots(7)$$

So that

$$\frac{X_R}{X_G} = \frac{A_6}{A_5} \quad \dots\dots\dots(8)$$

The area ratio, which is applied as a correction to X_G, is easily obtainable from consideration of isentropic expansion from conditions H_5, P_5 to H_6, P_6.

The expressions obtained are

Below the choke

$$(P_6 = P_0); \quad \frac{A_6}{A_5} = \left(\frac{P_5}{P_0}\right)^{\frac{1}{\gamma}} \left\{ \frac{1 - \left(\frac{P_5}{H_5}\right)^{\frac{\gamma-1}{\gamma}}}{1 - \left(\frac{P_0}{H_5}\right)^{\frac{\gamma-1}{\gamma}}} \right\}^{\frac{1}{2}} \quad \dots\dots\dots(9)$$

Above the choke

$$P_6 = \frac{H_5}{\left(\frac{\gamma+1}{2}\right)^{\frac{\gamma}{\gamma-1}}} ; \quad \frac{A_6}{A_5} = \left(\frac{\gamma+1}{2}\right)^{\frac{1}{\gamma-1}} \left(\frac{P_5}{H_5}\right)^{\frac{1}{\gamma}} \left\{ \frac{\gamma+1}{\gamma-1} \left[1 - \left(\frac{P_5}{H_5}\right)^{\frac{\gamma-1}{\gamma}} \right] \right\}^{\frac{1}{2}} \quad \dots(10)$$

/This applies

This applies to one dimensional flow. In the present tests the static pressure across the final nozzle exit is not uniform, so an equivalent mean static has been estimated, weighted for area. The error involved in weighting static pressure for area rather than integrating over the area of the jet is negligible since the total correction is of the order of a few per cent of thrust.

5. Consider now the single pitot method of thrust measurement in the light of the above discussion.

5.1 Using this method a pitot tube is fitted in the jet pipe upstream of the final nozzle and a calibration run on a test bed made in which this pitot value, H_4, and the static thrust, X_T, are measured over the r.p.m. range. The relation of $\dfrac{X_T}{P_o}$ v $\dfrac{H_4}{P_o}$ so obtained then provides a calibration for the uncowled static case of gross thrust against single pitot reading.

To apply this calibration to the installed flight case an 'effective area', A_f' is derived as a function of $\dfrac{H_4}{P_o}$* by inserting $H_4 = H_5$ and the measured value of X_T in equation (4) and assuming the classical theory values of P_5, so obtaining A_f' as the resulting value of A_5.

This effective area A_f', which may differ from the final nozzle area by up to the order of 10%, is regarded as a calibration of the single pitot which takes into account the discharge coefficient of the nozzle and any position error etc. of the tube.

In using it for the flight case it is therefore assumed that such factors are unchanged. Further, since much higher values of H_4/P_o are obtainable in flight at high altitude than on the ground calibration run the curve of A_f' v $\dfrac{H_4}{P_o}$ must be extrapolated and this is done on the assumption that A_f' is constant above the critical value of $\dfrac{H_4}{P_o} = \left(\dfrac{\gamma + 1}{2}\right)^{\frac{\gamma}{\gamma-1}}$ after which sonic conditions obtain at the nozzle; this value is usually just reached on the test bed run.

5.2 Errors in the derived thrust may thus arise from the following causes.

(1) A change in the relation between single pitot reading H_4 and mean final nozzle total pressure / H_5 due to the different intake conditions resulting from installation in the aircraft and to Reynolds number effects. These effects may cause differences between the ground installed and flight cases.

(2) A change in the exit static pressure, i.e. in the relation P_5/P_o v H_4/P_o between the test bed and flight cases; this would correspond to a different contraction ratio A_6/A_5 behind the nozzle. It would be expected that with increasing flight speed (or V_o/V_5) the external flow would cause an increasing contraction and hence a higher static pressure than that on the test bed, which is assumed to still apply in the application of the single pitot calibration.

(3) If (as has been found for the Derwent 5) the total and static pressures are non-uniform in the final nozzle, the nozzle flow does not become uniformly sonic at

$$\frac{H_4}{P_o} = \left(\frac{\gamma + 1}{2}\right)^{\frac{\gamma}{\gamma-1}} = 1.85 ;$$

in this particular case the critical pressure ratio was not reached at the centre of the nozzle until $H_4/P_o \sim 2.4$. The flow distribution thus does not remain uniform above the critical value of H_4/P_o and the effective area for the single pitot cannot be assumed to remain constant in this region.

_____

* It has sometimes in the past been the practice to regard A_f' as a function of $N/\sqrt{\theta_1}$; H_4/P_o is however now regarded as the more relevant parameter and this is supported by Figs. 16 and 17.

Appendix 2

Method of deriving thrust from pitot static rake measurements

1. ## Calculation of rake thrust, X_G

It is shown in Appendix 1 that

$$X_R = X_G \frac{A6}{A_5} \qquad \dots\dots\dots(1)$$

The factor $\frac{A6}{A_5}$ is obtained from the static pressure in the final nozzle as in paragraph 5 of this Appendix.

From Appendix 1

$$\frac{X_G}{A_5} = x_G = \frac{2}{\gamma - 1} P_5 \left[\left(\frac{H_5}{P_5}\right)^{\frac{\gamma-1}{\gamma}} - 1 \right] + (P_5 - P_0) \qquad \dots\dots\dots(2)$$

where $P_5 = P_0$ or $\dfrac{H_5}{\left(\frac{\gamma+1}{2}\right)^{\frac{\gamma}{\gamma-1}}}$ whichever is the greater.

Then taking $\gamma = 4/3$

$$\frac{x_G}{P_0} = 8 \left[\left(\frac{H_5}{P_0}\right)^{\frac{1}{4}} - 1 \right] \qquad \dots\dots\dots(3)$$

$$\text{below the critical value of } \frac{H_5}{P_0} = 1.85$$

and

$$\frac{x_G}{P_0} = 1.259 \frac{H_5}{P_0} - 1 \qquad \dots\dots\dots(4)$$

$$\text{above this value.}$$

From equations (3) and (4) above a plot can be made of $\dfrac{x}{P_0}$ against $\dfrac{H_5}{P_0}$

Hence for each pitot value of H_5/P_0 the thrust per unit area x/P_0 can be obtained from the plot.

Then, considering a pitot at radius r the value of $\dfrac{\text{thrust}}{P_0}$ for the annulus width δr at that radius, assuming uniform circumferential distribution, will be

$$2\pi \, r.\delta r \ . \ \frac{x_G}{P_0}$$

and over the whole area of the final nozzle

$$\frac{X_G}{P_0} = \frac{2\pi}{P_0} \int_0^R x_G \, r. \, dr$$

The integral $\displaystyle\int_0^R x_G \, r. \, dr$ can be conveniently obtained by a graphical method, each product being plotted at the corresponding radius. The boundary layer is at this stage neglected, and a correction made later. The area under the resulting curve is the required integral.

2. ## Correction to thrust for boundary layer in final nozzle

The total head at three positions close to the final nozzle wall (1/16, 3/16, $\frac{1}{4}$ inch) was obtained over a range of r.p.m. during a ground run.

The corresponding values of x.r have been plotted in several of the graphical integrations and the mean value for the loss in thrust due to the boundary layer found. This is equivalent to a decrease in final nozzle area of 1.9%. This correction has been made to all rake results.

3. Correction for expansion of final nozzle

It has been assumed that the increase in area of the final nozzle due to expansion was 1.3%. This figure is based on a final nozzle temperature of 500°C, coefficient of expansion 13×10^{-6} ft/ft/°C. This will be the approximate temperature at maximum r.p.m. The error at other speeds will be very small. (This is the value used by Messrs. Rolls Royce in similar work - Ref.9)

4. Correction of thrust to nominal $V_i/\sqrt{P_o}$

The variation of aircraft speed from the nominal value was not negligible in some of the tests, especially at the higher altitudes, and a correction has been derived using information from the Rolls Royce Derwent 5 brochure (Ref.10).

The thrust over a range of $N/\sqrt{\theta_1}$ was established from the non dimensional thrust curve for the various nominal test conditions and at airspeeds above and below the nominal test conditions.

The variation of thrust with speed was then assumed to be linear over the small intervals considered, and the differential $\dfrac{V}{X} \dfrac{\partial X}{\partial V}$ calculated.

Each flight thrust measurement has been corrected to the nominal test airspeed using this information. The largest correction involved was 2.7% of thrust, but the mean correction was 0.9%.

Single pitot thrust values have also been corrected in this way, and the corrected total head corresponding to this corrected thrust is tabulated and used in this report.

5. Static pressure correction

This is applied as the factor $\dfrac{A_6}{A_5}$ in equation (1) of this Appendix. $\dfrac{A_6}{A_5}$ is derived as a function of $\dfrac{P_5 - P_o}{P_o}$ and $\dfrac{H_5}{P_o}$ in Appendix 1 and plotted in Fig.14.

In deriving this parameter the static pressure in the final nozzle is taken to be uniform and in applying it for the measured static pressures an equivalent uniform static pressure was first obtained as the mean of the observed distribution weighted for area.

In the flight tests static pressures were only measured at the centre and wall of the final nozzle (Fig.13). Intermediate positions were obtained on ground runs however (Fig.12) and the required mean for these readily obtainable. For the flight results the static pressure variation across the nozzle was assumed to be similar and the mean value taken to bear the same relation to the centre and wall values as on the ground runs.

The corrections derived in this way, which have been applied to the rake thrust X_G to give the fully corrected rake thrust X_R, are shown in Fig.15 for the ground and flight conditions at which the tests were made.

A check has been made on the accuracy of taking a mean static pressure weighted for area. This was done by using Fig.14 to correct the value of thrust per unit area derived from each of the single pitots for the measured static pressure at that radius, and integrating the resultant values across the final nozzle area. The thrust correction thus derived was in good agreement with that given by the simpler method used.

Appendix 3

Possible sources of observed scatter in thrust
derived from total pressure measurements

1. Differential pressure gauge

The instrument selected for the pressure measurements in these tests was a two pointer sensitive differential pressure gauge of range -3 to +20 lb/sq.in.

The gauge is temperature compensated and the auto-observer was heated, the temperature being usually between 5 and 15°C. The instruments used were frequently calibrated and no sudden changes in instrument error encountered.

The mean lag* was about 0.03 and the maximum 0.10 lb/sq.in. The gauge could be read to a nominal 0.02 lb/sq.in. The accuracy of the gauge would be expected to be about 0.1 lb/sq.in.

The pressure ranges required were as follows:

Ground run	2.3 - 10	lb/sq.in.
5,000 ft.	2.4 - 12	lb/sq.in.
40,000 ft.	1.5 - 4.3	lb/sq.in.

The error in thrust for a 1% error in dynamic pressure is given in Table 9 and is approximately 0.9% over the working range of total head values.

Thus for the ground runs and 5,000 ft. flights the instrument errors should not cause random scatter of any significance. At high altitude however the maximum error of a single observation could be 6% at the lowest total pressure decreasing to 2% at the higher values.

In any future single pitot and rake measurements the use of an accurate pressure gauge of a smaller range is recommended for high altitude measurements in conjunction with a gauge of the type used for use at low altitude. Some automatic switching device might be necessary to protect the low range instrument from high pressures at low altitudes. It is possible that an A.S.I. with a suitable pressure range could be used at high altitudes.

2. Engine speed indicators

The accuracy of these instruments is quoted as 1% of full range corresponding to a possible 1½% error at high r.p.m. Since the change of thrust for one per cent change in r.p.m. rises to about 3½% at high r.p.m., this could introduce a scatter in the results comparable with that possible from the pressure gauge at high altitude.

The actual scatter of the thrust values obtained is of the order of 8% throughout the total head range at 40,000 ft. and about 2% at 5,000 ft. This latter figure can be considered satisfactory when these two possible sources of error are considered but the increase in scatter at 40,000 ft. then seems excessive.

3. Other sources of error

Other possible sources of error in the tests are in the unsteadiness of flight conditions during the period when a set of readings was being taken and possible malfunctioning of the selector box.

/3.1

---

*Defined as difference in reading of a vibrated instrument at the same applied differential pressure calibrating first with differential pressure increasing and then decreasing.

3.1 During a set of readings some variation in A.S.I., height and r.p.m. did in fact occur, particularly at high altitude. However during the 30 second reading period each pressure was read 3 times at 10 second intervals and the mean value was ascribed to the mean flight conditions so that the final error involved would be considerably less than that due to the overall change. The biggest change was in r.p.m. where the mean variation during a set of readings was 40 and the maximum 100. The resultant error should generally be negligible.

3.2 A further source of error in the pitot rake results is the selector box. It will be seen from Fig.18 that the scatter of the thrust values at 35,000 feet, estimated from the rake, is rather higher than those from the single pitot. This may be, in part at least, due to malfunctioning of the selector. This was ground checked at intervals for satisfactory operation of the valves but their continued satisfactory operation at high altitude could not be entirely verified. A check was made however on the initial flights by duplicating the pressure recorded at one rake pitot as a continuous reading on another gauge and satisfactory agreement with the selector gauge found. On several occasions a tube was found to be giving grossly inconsistent readings, the trouble being located in a faulty valve which was rectified. On such occasions the relevant pressure was obtained by interpolation from the adjacent tubes, if the faulty tube was one of those near the centre where pressure errors would contribute little to errors in the integrated thrust value. Otherwise a repeat test was made.

While some such device is necessary for these measurements in an aircraft where auto-observer space is restricted it would be very desirable where possible in such tests to have a separate gauge for each tube or, if only mean total pressure is required for thrust estimation and not necessarily the actual distribution, to use an integrating rake recording continuously on a single gauge (Ref.11).

Derivation of the function $\dfrac{\dfrac{X}{A_f\ P_0} + 1}{R_{01}}$

The usual non dimensional theory states that the non dimensional thrust is a function only of $\dfrac{N}{\sqrt{\theta_1}}$ and the ram ratio $\dfrac{P_1}{P_0}$. In order to compare the gross thrust of an engine measured in flight over a range of $\dfrac{N}{\sqrt{\theta_1}}$ at several ram ratios $\dfrac{P_1}{P_0}$, to check the validity of the above assumption, it is desired to find some function of the gross thrust which is independant of the ram ratio and varies only with $\dfrac{N}{\sqrt{\theta_1}}$.

This can be done above the final nozzle choke as follows:

Consider an engine, on a stand, running at or above the choke, there being an evenly distributed pressure P_1 corresponding to the ram pressure around the intake and engine, the engine exhausting to a pressure P_0.

Then if the choke occurs at the final nozzle the force F measured on the stand will be

$$F = \frac{M_5\ v_5}{g} + A_f\ (P_5 - P_0) - A_f\ (P_1 - P_0)$$

Assuming zero intake momentum

Therefore $\dfrac{F}{A_f\ P_1} = \dfrac{M_5\ v_5}{P_1}\ \dfrac{1}{g\ A_f} + \dfrac{P_5}{P_1} - 1$ ....(1)

At pressure ratios above that at which the final nozzle chokes P_5 and $M_5\ v_5$ are directly proportional to P_1, so that at any particular $\dfrac{N}{\sqrt{\theta_1}}$ the expression $\dfrac{F}{A_f\ P_1}$ will be unique for any P_1 and independent of P_0.

Now the gross thrust $X = \dfrac{M_5\ v_5}{g} + A_f\ (P_5 - P_0)$

$\therefore\ \dfrac{F}{A_f\ P_1} = \dfrac{X}{A_f\ P_1} - \left(\dfrac{P_1 - P_0}{P_1}\right) = \dfrac{\dfrac{X}{A_f\ P_0} + 1}{R_{01}} - 1$, where $R_{01} = \dfrac{P_1}{P_0}$

which from (1) is independent of R_{01} above the choke

Hence $\dfrac{\dfrac{X}{A_f\ P_0} + 1}{R_{01}}$ is independent of $\dfrac{P_1}{P_0}$

above the choke, and when plotted against $\dfrac{N}{\sqrt{\theta_1}}$ the values of this function should lie on a unique curve if the assumptions of the non-dimensional theory are correct. Below the choke measurements at various ram ratios should be on a series of unique curves.

In practice the function is plotted as $\dfrac{\dfrac{X}{A_f^1 P_0} + 1}{R_{01}}$, This being a

convient form when the single pitot effective area A_f^1 is assumed constant above the choke.

/Then....

Then by the momentum theory $\dfrac{X}{A_f{}^1 P_0} = 1.259 \dfrac{H_4}{P_0} - 1$ (Appendix 2)

and we have

$$\dfrac{\dfrac{X}{A_f{}^1 P_0} + 1}{R_0{}^1} = 1.259 \dfrac{H_4}{P_1} .$$

In this case a value of $A_f{}^1 = 188$ sq. ins. has been used when plotting this function, this corresponding closely to the value of the effective area of 187 sq. ins. obtained for the test engine at the choke (Fig. 3) and being the value used in the Rolls Royce brochure in the plot of this function as being a typical value of the effective area.

Test	hp.feet	$N/\sqrt{\theta_1}$	$V_1/\sqrt{P_o}$	(H_4/P_o)	$\frac{\chi GP}{P_o}$	$\frac{\chi GP}{P_o}$	H_4/P_o	Using test bed $\Delta f'$ XGP/P_o	XG'/P_o	XG/P_o	$\chi G/P_o$	$\bar{H}_5/P_o$	$H_4/\bar{H}_5$	Rake $\Delta f'$	XR/P_o
Ground	--	10,000	--	--	--	45.0	1.166	64.8	--	67.1	47.5	1.1758	0.992	1.463	65.8
"	--	10,500	--	--	--	53.4	1.199	75.8	--	77.1	54.6	1.204	0.996	1.416	75.6
"	--	11,000	--	--	--	62.0	1.233	86.9	--	85.7	60.6	1.228	1.004	1.355	84.0
"	--	11,500	--	--	--	70.8	1.270	98.5	--	97.7	69.2	1.263	1.005	1.353	95.7
"	--	12,000	--	--	--	81.0	1.313	112.3	--	109.7	77.6	1.298	1.012	1.332	107.9
"	--	12,500	--	--	--	92.6	1.363	125.6	--	125.1	88.6	1.346	1.013	1.328	123.0
"	--	13,000	--	--	--	107.3	1.429	141.2	--	138.3	97.9	1.387	1.030	1.268	136.0
"	--	13,500	--	--	--	124.0	1.507	161.2	--	155.4	110.0	1.442	1.045	1.235	153.1
"	--	14,000	--	--	--	141.2	1.590	182.4	--	176.5	125.0	1.511	1.052	1.231	174.0
"	--	14,250	--	--	--	150.5	1.635	194.1	--	185.5	131.3	1.542	1.060	1.215	182.9
5.aA.1.1	5000	9,300	262.3	1.181	48.8	48.7	1.180	69.7	76.4	76.3	54.0	1.202	0.982	1.482	72.1
2	4870	10,280	264.0	1.240	63.7	63.5	1.240	88.8	96.7	96.5	68.3	1.260	0.984	1.460	92.6
3	5000	11,290	264.0	1.331	85.1	84.8	1.330	115.2	119.7	119.3	84.4	1.328	1.002	1.369	116.0
4	5220	12,290	264.9	1.468	115.8	115.3	1.466	150.6	149.7	149.0	105.5	1.420	1.032	1.264	145.7
5.aA.2.1	5150	9,250	262.0	1.181	48.8	48.7	1.181	69.7	74.0	73.9	52.3	1.195	0.989	1.435	69.8
2	5060	10,290	262.0	1.231	61.2	61.1	1.230	85.7	94.2	94.0	66.5	1.252	0.982	1.478	90.2
3	5100	11,210	259.0	1.330	85.0	85.1	1.331	117.3	121.2	121.4	86.0	1.335	0.997	1.389	118.1
4	4990	12,220	262.0	1.441	109.7	109.5	1.440	143.9	144.6	144.4	102.1	1.405	1.024	1.290	141.3
5.aA.3.1	5040	9,250	264.9	1.182	49.1	48.9	1.1815	69.9	75.2	74.9	53.0	1.197	0.987	1.446	70.7
2	5055	10,250	264.9	1.252	66.3	66.0	1.250	92.1	91.3	90.9	64.3	1.243	1.006	1.320	87.0
3	5020	11,250	264.0	1.337	86.4	86.1	1.335	118.6	116.2	115.8	82.1	1.318	1.013	1.305	112.4
4	4960	12,250	264.0	1.452	112.3	111.9	1.450	146.7	148.0	147.5	104.4	1.417	1.023	1.290	144.1
5.bA.1.1	4820	11,230	416.0	1.465	115.1	114.4	1.462	149.7	150.4	149.4	105.5	1.421	1.029	1.240	142.0
2	5430	12,290	421.3	1.662	155.8	153.5	1.651	198.1	197.5	194.5	137.7	1.573	1.049	1.227	188.3
3	5260	13,290	419.5	1.867	194.0	191.7	1.854	249.4	249.7	246.7	174.5	1.760	1.054	1.266	242.4
5.bA.2.1	5380	11,275	418.6	1.480	118.5	117.3	1.474	153.1	157.2	155.6	110.1	1.443	1.021	1.264	148.2
2	5550	12,210	422.0	1.644	152.4	150.0	1.633	193.9	196.9	193.7	137.1	1.570	1.041	1.250	187.5
3.3	5315	13,120	418.6	1.824	186.2	184.2	1.813	239.6	240.1	237.5	168.1	1.726	1.050	1.265	233.0
3.4	5420	14,120	420.4	2.105	237.2	233.9	2.086	304.0	301.9	297.7	210.6	1.958	1.065	1.267	296.0
40.bA.1.1	39570	11,220	411.7	1.475	117.4	117.6	1.476	153.5	151.4	151.6	107.3	1.430	1.032	1.209	142.1
2	39560	12,230	411.7	1.636	150.6	150.8	1.637	194.8	188.4	188.7	133.5	1.553	1.054	1.199	180.8
3	39540	13220	411.7	1.802	182.4	182.7	1.805	235.9	232.5	233.0	165.0	1.710	1.055	1.249	228.0
4	39670	14,290	419.5	2.075	231.9	229.1	2.060	297.9	293.8	290.3	205.5	1.930	1.068	1.260	288.3
40.bA.2.3	39820	13,390	417.8	1.915	202.8	201.0	1.905	261.3	248.7	246.5	174.5	1.762	1.082	1.206	242.3
4	39900	14,210	413.4	2.077	232.2	231.9	2.076	301.3	280.6	280.2	193.4	1.891	1.097	1.198	277.8
40.cA.1.1	39400	13,180	485.0	1.950	209.0	206.2	1.933	268.0	266.9	263.3	186.4	1.825	1.059	1.257	259.3
2.2	40260	14,230	489.0	2.236	261.0	256.0	2.208	333.0	328.7	322.3	228.0	2.054	1.075	1.255	321.0
40.cA.2.3	40,120	15,260	482.0	2.540	316.0	313.6	2.527	407.0	393.0	390.0	276.0	2.320	1.090	1.241	339.0
2.4	40090	15,895	484.0	2.738	351.8	347.7	2.715	451.0	444.7	439.5	311.0	2.512	1.081	1.260	438.0

Test	hp.feet	$N/\sqrt{\theta_1}$	$Vi/\sqrt{po}$	$(H_4/Po)'$	$\dfrac{xGP'}{Po}$	$\dfrac{xGP}{Po}$	H_4/Po'	Using test bed Af' xGP/Po	xG'/Po	xG'/Po	xG/Po	$\bar{H}_5/Po$	$H_4/\bar{H}_5$	Rake Af'	XR/Po
Ground	–	10,000	–	–	–	43.8	1.162	63.1	–	67.5	47.8	1.177	0.987	1.512	66.2
"	–	10,500	–	–	–	52.4	1.195	74.6	–	74.7	52.9	1.197	0.998	1.398	73.2
"	–	11,000	–	–	–	61.5	1.232	86.2	–	82.8	58.6	1.220	1.009	1.320	81.1
"	–	11,500	–	–	–	69.3	1.263	96.5	–	95.8	67.8	1.257	1.005	1.355	93.9
"	–	12,000	–	–	–	79.1	1.305	109.8	–	109.3	77.4	1.298	1.005	1.359	107.4
"	–	12,500	–	–	–	91.8	1.360	124.7	–	122.8	87.0	1.339	1.016	1.314	120.6
"	–	13,000	–	–	–	105.5	1.421	139.4	–	138.9	98.3	1.389	1.023	1.294	136.5
"	–	13,500	–	–	–	122.7	1.502	159.5	–	158.0	111.8	1.450	1.036	1.269	155.7
"	–	14,250	–	–	–	148.7	1.627	192.0	–	185.0	130.9	1.540	1.056	1.226	182.1
5.aB.1.3.	5000	11,250	259.7	1.328	84.5	84.6	1.328	116.7	116.3	116.4	82.4	1.320	1.006	1.335	113.0
4	5100	12,250	261.4	1.456	113.0	112.9	1.455	147.9	149.1	149.0	105.5	1.422	1.023	1.291	145.8
5.bB.1.1	5220	11,250	416.0	1.465	115.2	114.5	1.463	149.8	155.8	154.9	109.6	1.440	1.016	1.289	147.5
2	5470	12,250	418.6	1.647	152.8	151.2	1.639	195.1	197.2	195.1	138.2	1.575	1.040	1.250	189.0
3	5320	13,235	418.6	1.877	196.0	194.0	1.867	252.2	253.2	250.6	177.4	1.775	1.052	1.270	246.2
4	5270	14,035	417.0	2.083	233.3	231.6	2.074	301.1	302.9	300.8	212.8	1.970	1.053	1.294	299.5
40.bB.1.3	39870	13,390	404.8	1.838	188.8	191.3	1.852	249.0	237.6	240.8	170.4	1.739	1.065	1.234	236.0
4	39930	14,210	422.0	2.055	228.2	224.4	2.033	291.7	268.7	283.9	200.8	1.904	1.068	1.252	281.0
40.cB.1.2	40050	14,230	473.2	2.170	249.0	250.9	2.181	326.0	302.2	304.5	215.5	1.985	1.099	1.209	303.0

TABLE 4

RAKE POSITION 'C'

Test	hp.feet	$N/\sqrt{\theta_t}$	$V_1/\sqrt{Po}$	$(H_4/Po)'$	$\dfrac{X'GP}{Po}$	$\dfrac{\Sigma GP}{Po}$	H_4/Po	Using test bed Af' XGP/Po	X'_G/Po	XG/Po	YG/Po	$\bar{H}_5/Po$	H_4/H_5	Rake Af'	XR/Po
Ground	–	10,150	–	–	–	46.8	1.173	67.15	–	66.5	47.1	1.174	0.999	1.393	65.2
"	–	10,640	–	–	–	52.6	1.196	74.8	–	76.8	54.4	1.203	0.994	1.432	75.3
"	–	11,160	–	–	–	62.3	1.235	87.2	–	87.2	61.7	1.232	1.002	1.373	85.5
"	–	11,670	–	–	–	71.8	1.274	100.0	–	98.9	70.0	1.266	1.006	1.350	96.9
"	–	12,130	–	–	–	81.4	1.316	112.7	–	113.2	80.2	1.310	1.004	1.370	111.4
"	–	12,650	–	–	–	92.8	1.364	125.7	–	127.8	90.4	1.353	1.008	1.352	125.5
"	–	13,200	–	–	–	110.8	1.445	145.4	–	145.4	102.9	1.410	1.025	1.291	143.0
"	–	13,690	–	–	–	129.0	1.530	167.3	–	165.6	117.2	1.475	1.037	1.265	163.1
"	–	14,210	–	–	–	147.7	1.622	190.75	–	186.5	132.0	1.545	1.050	1.244	183.8
"	–	14,630	–	–	–	163.0	1.700	210.2	–	206.6	146.2	1.614	1.053	1.252	204.0
5.aC.1.3	5110	11,240	264.0	1.326	85.8	83.5	1.325	115.4	117.8	117.4	83.1	1.322	1.002	1.363	113.8
4	5170	12,260	264.9	1.467	115.7	115.2	1.456	150.6	152.8	152.1	107.7	1.431	1.025	1.291	148.9
5.bC.1.1	4990	11,140	417.0	1.453	112.5	111.7	1.449	146.4	153.4	152.2	107.75	1.431	1.013	1.295	144.6
2	5370	12,260	420.4	1.656	154.5	152.4	1.644	196.6	201.8	199.1	141.0	1.589	1.035	1.269	193.1
3	5650	13,270	420.4	1.869	194.6	192.0	1.855	249.6	255.8	252.3	178.6	1.782	1.041	1.297	248.8
4	5640	14,250	420.4	2.144	244.0	240.7	2.124	312.9	318.1	313.8	222.0	2.021	1.051	1.300	312.8
35.bC.2.1	35360	11,260	423.0	1.488	120.0	117.8	1.477	153.7	162.6	159.7	113.0	1.455	1.015	1.279	150.5
2	35200	12,140	421.3	1.635	150.4	148.1	1.624	191.2	196.5	193.5	137.0	1.570	1.034	1.255	185.9
3	35305	13,180	417.0	1.784	179.0	177.7	1.777	229.7	226.7	225.0	159.2	1.680	1.057	1.235	219.4
4	35195	14,270	417.0	2.050	227.3	225.6	2.041	293.2	292.7	290.5	205.7	1.931	1.057	1.280	288.5
35.cC.2.1	35460	13,190	493.2	1.955	210.0	206.8	1.937	268.7	279.6	275.6	195.0	1.870	1.037	1.315	272.0
2	35390	14,210	487.1	2.250	263.5	259.1	2.225	336.9	340.3	334.7	236.8	2.103	1.058	1.290	334.0
3	35340	15,190	482.9	2.534	315.0	312.2	2.519	405.7	412.8	409.1	289.6	2.395	1.052	1.308	408.0
4	35470	15,800	493.2	2.784	360.0	354.6	2.754	460.9	476.1	463.2	328.0	2.607	1.057	1.306	463.2
40.bC.1.4	39990	14,300	415.2	2.095	235.4	234.3	2.089	304.6	303.4	302.0	213.8	1.976	1.057	1.282	300.5

Test	hp.feet	$I\sqrt{\theta_1}$	$V_1\sqrt{Po}$	$(H_4/Po)'$	$\dfrac{\Sigma GP'}{Po}$	$\dfrac{\Sigma GP}{Po}$	H_4/Po	Using test bed Af' $\Sigma GP/Po$	XG'/Po	XG/Po	YG/Po	$\bar{H}_5/Po$	$H_4/\bar{H}_5$	Rake Af'	AR/Po
Ground	–	10070	–	–	–	43.8	1.162	63.1	–	68.2	48.6	1.180	0.985	1.526	66.8
"	–	10620	–	–	–	53.6	1.200	76.1	–	74.6	52.8	1.197	1.003	1.365	73.1
"	–	11130	–	–	–	63.8	1.241	89.2	–	86.8	61.4	1.232	1.008	1.334	85.0
"	–	11620	–	–	–	71.0	1.271	98.85	–	97.6	69.1	1.263	1.006	1.349	95.6
"	–	12170	–	–	–	81.9	1.317	113.4	–	112.7	79.6	1.307	1.007	1.355	110.9
"	–	12630	–	–	–	95.0	1.374	128.0	–	127.3	90.3	1.353	1.016	1.318	125.1
"	–	13190	–	–	–	114.0	1.460	149.1	–	145.4	102.6	1.408	1.037	1.255	143.0
"	–	13670	–	–	–	130.4	1.537	168.9	–	163.9	116.2	1.470	1.045	1.240	161.5
"	–	14210	–	–	–	150.8	1.637	194.8	–	186.4	131.9	1.544	1.061	1.219	183.6
"	–	14570	–	–	–	164.0	1.705	211.5	–	205.7	145.5	1.611	1.059	1.238	203.0
5.aB'.1.3	5120	11250	262.3	1.325	33.7	83.6	1.326	115.6	114.8	114.6	81.1	1.314	1.010	1.330	111.2
4	5130	12250	261.4	1.450	111.9	111.8	1.451	146.6	148.3	148.2	104.8	1.418	1.024	1.298	145.0
5.bB'.1.1.	5310	11200	418.6	1.464	115.0	113.8	1.459	149.0	154.1	152.5	107.9	1.432	1.019	1.275	145.0
2	5290	12180	419.5	1.641	151.7	149.9	1.633	193.5	194.2	191.9	135.8	1.564	1.045	1.240	185.8
3	5300	13160	419.5	1.856	192.1	189.8	1.843	246.7	248.0	245.1	173.5	1.755	1.051	1.271	241.0
4	5420	14220	419.5	2.130	241.7	238.8	2.114	310.3	314.0	310.3	219.6	2.007	1.054	1.300	310.0
35.bB'.1.1	34780	11220	417.0	1.494	121.4	120.5	1.490	156 8	156.2	155.0	109.7	1.441	1.034	1.210	145.8
2	35260	12210	422.0	1.652	153.8	151.3	1.639	195.3	189.4	186.3	131.9	1.545	1.061	1.176	178.0
3	35330	13220	421.3	1.832	187.7	184.9	1.817	239.7	228.9	225.5	159.6	1.682	1.080	1.190	220.0
4	35020	14310	417.8	2.052	227.7	225.7	2.042	293.3	286.0	283.5	200.3	1.900	1.076	1.245	280.5
35.cB'.1.1	35220	13050	484.5	1.913	202.6	200.2	1.901	260.2	255.3	252.3	178.6	1.783	1.066	1.236	247.5
2	35330	14170	478.5	2.197	253.8	253.4	2.195	329.4	323.1	322.6	223.3	2.055	1.069	1.269	321.0
3	35360	15110	484.5	2.537	315.4	311.6	2.516	404.9	397.1	392.6	277.9	2.330	1.030	1.259	392.0

Table 6

Derwent 5
Engine No. 4045

Rolls Royce
Turbine Test Dept.
18.11.49.
Ref: Lov/FG/LH 2/OT

Po = 29.59" Hg.

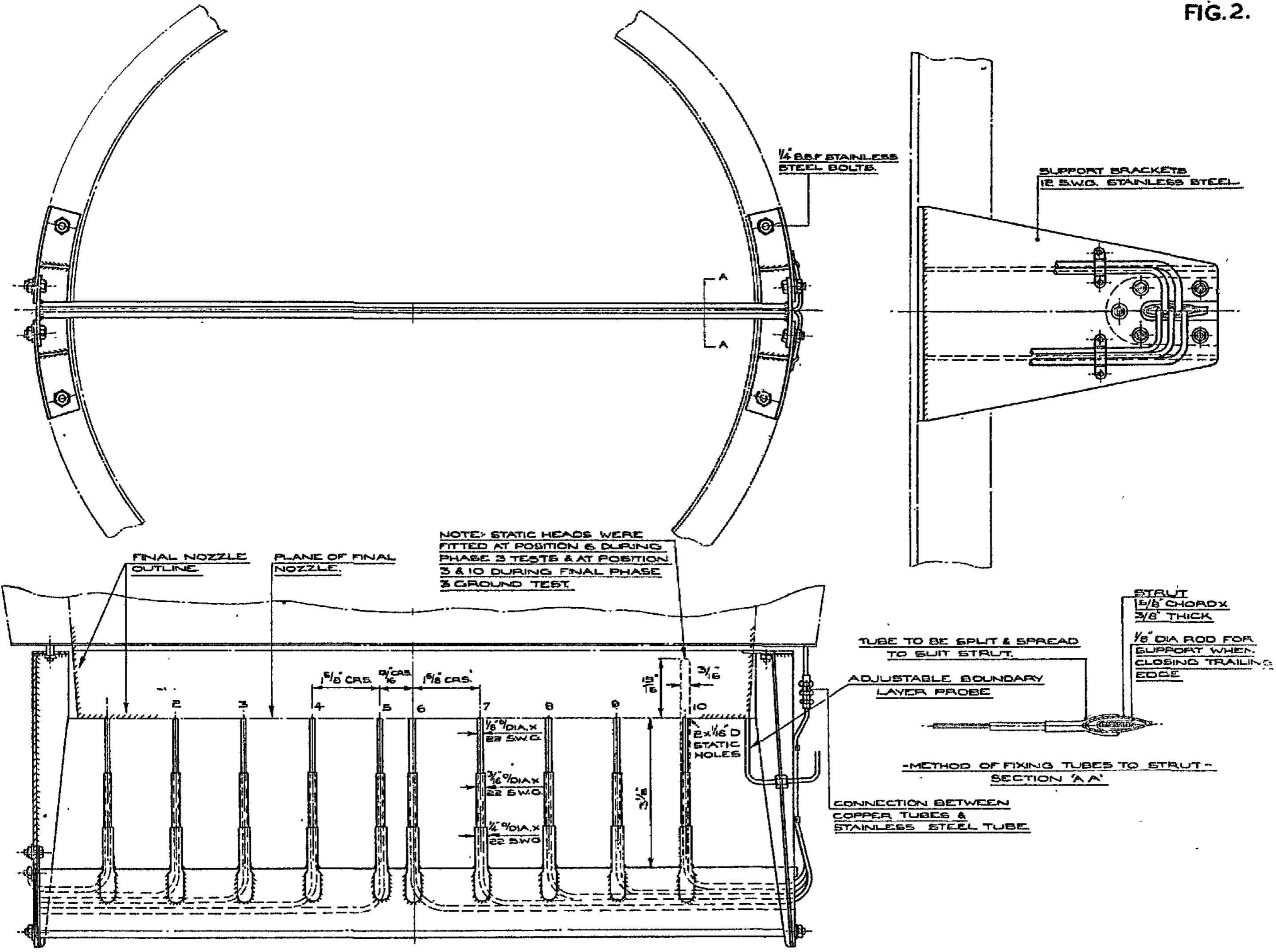| $N/\sqrt{\theta_1}$	H_4-P_o	H_4/P_o	$\dfrac{YGP}{P_o}$	$\dfrac{XT}{lb.}$	XT/P_o	$A_f{}'$	$\dfrac{YT}{P_o}$	$\dfrac{\bar{H}_T}{P_o}$	$\dfrac{H_4}{\bar{H}_T}$
	Inches Hg.			Thrust Measured					
10110	5.20	1.1758	47.52	985	67.85	1.428	48.05	1.178	0.998
10610	6.10	1.2061	55.11	1135	78.05	1.417	55.25	1.207	0.999
11120	7.12	1.2405	63.63	1290	88.8	1.395	62.85	1.237	1.004
11620	8.35	1.2821	73.60	1488	102.2	1.390	72.35	1.277	1.004
12130	9.85	1.3325	85.49	1710	117.8	1.378	83.4	1.324	1.007
12630	12.08	1.408	102.64	1976	136.0	1.328	96.25	1.379	1.021
13130	14.40	1.486	119.62	2267	156.0	1.307	110.4	1.444	1.028
13630	17.30	1.585	140.24	2645	182.2	1.299	129.0	1.531	1.036
14140	20.20	1.683	159.69	2993	205.9	1.290	145.75	1.613	1.044
14630	23.65	1.800	181.86	3421	235.8	1.297	166.9	1.720	1.047
14830	25.15	1.8495	190.9	3603	248.0	1.302	175.6	1.767	1.048
14630	23.65	1.800	181.86	3416	234.6	1.292	166.0	1.714	1.050
14120	20.22	1.6845	159.99	2995	206.0	1.289	145.8	1.613	1.045
13630	17.51	1.592	141.58	2643	182.0	1.288	128.9	1.530	1.041
12620	12.00	1.4055	102.07	1971	135.8	1.329	96.1	1.378	1.020
12120	9.80	1.3316	85.29	1712	117.9	1.381	83.4	1.324	1.005
11610	8.35	1.2821	73.60	1493	102.8	1.395	72.75	1.278	1.003
11110	7.05	1.2381	63.04	1285	88.45	1.401	62.6	1.237	1.001
10600	6.08	1.2055	54.97	1133	78.0	1.420	55.2	1.207	0.998
10100	5.15	1.1740	47.05	983	67.6	1.438	47.85	1.177	0.998
				Repeat					
10080	5.12	1.1738	47.00	983	67.9	1.443	48.05	1.178	0.997
11100	7.05	1.2392	63.29	1285	88.6	1.402	62.7	1.237	1.002
12110	9.75	1.3302	84.93	1700	117.4	1.383	83.05	1.322	1.007
13110	14.28	1.4845	119.30	2253	155.2	1.301	109.8	1.442	1.030
14120	20.00	1.6785	158.80	2981	206.0	1.299	145.8	1.613	1.042
14840	25.00	1.8485	190.73	3593	248.0	1.301	175.6	1.767	1.047
14630	23.50	1.796	181.11	3403	235.2	1.298	166.5	1.718	1.045
13620	17.30	1.5865	140.55	2625	181.3	1.292	128.3	1.528	1.038
12610	11.90	1.404	101.74	1963	135.7	1.334	96.05	1.378	1.019
11600	8.11	1.2752	72.02	1485	102.5	1.423	72.55	1.278	0.998
10590	6.00	1.2036	54.51	1115	77.0	1.412	54.5	1.204	0.999
14710	23.95	1.8105	183.50	3468	239.6	1.304	169.6	1.736	1.043

Table 9

H_5/P_o	Percentage change in thrust for 1% change in (H_5/P_o)	% Change in thrust for 1% change in $\dfrac{H_5}{H_5 - P_o}$
1.15	7.20	.939
1.20	5.60	.933
1.30	3.90	.900
1.40	3.10	.886
1.60	2.25	.844
1.80	1.82	.809
2.20	1.56	.853
2.60	1.44	.886

FIG. I.

SCRAP SECTION - FINAL NOZZLE.

STREAMLINE STRUT 1/2" X 3 1/4".
STATIC HOLES IN TUBE 2 X 1/16 D.
TO DIFFERENTIAL PRESSURE GAUGE

5 1/2°
9"
30·5'
65·7'
1·62
1 1/2" D
SINGLE PITOT.
JET PIPE FLANGE
18·0 DIA.
1/2"
TURBINE EXHAUST CONE
22 1/2'
A

₵ OF WALLSTATIC.
18·11 DIA.
16·0 DIA.
7/32"
·15
1·72
·16
·13
16·42 DIA.
·05
16·34 DIA.
16·50 DIA.
17·78 DIA.

RAKE POSITION C.
SINGLE PITOT POSITION.
RAKE POSITION A
RAKE POSITIONS B & B'
18°
2
1
3
4
VIEW ON ARROW 'A'

NOTE: WALL STATICS FITTED AT POSITIONS 1,2,3, AND 4.

JET PIPE & FINAL NOZZLE LAYOUT & INSTALLATION OF LONG TUBE FOR STATIC CALIBRATION.

FIG.2.

GENERAL ARRANGEMENT OF PITOT RAKE.

FIG.3.
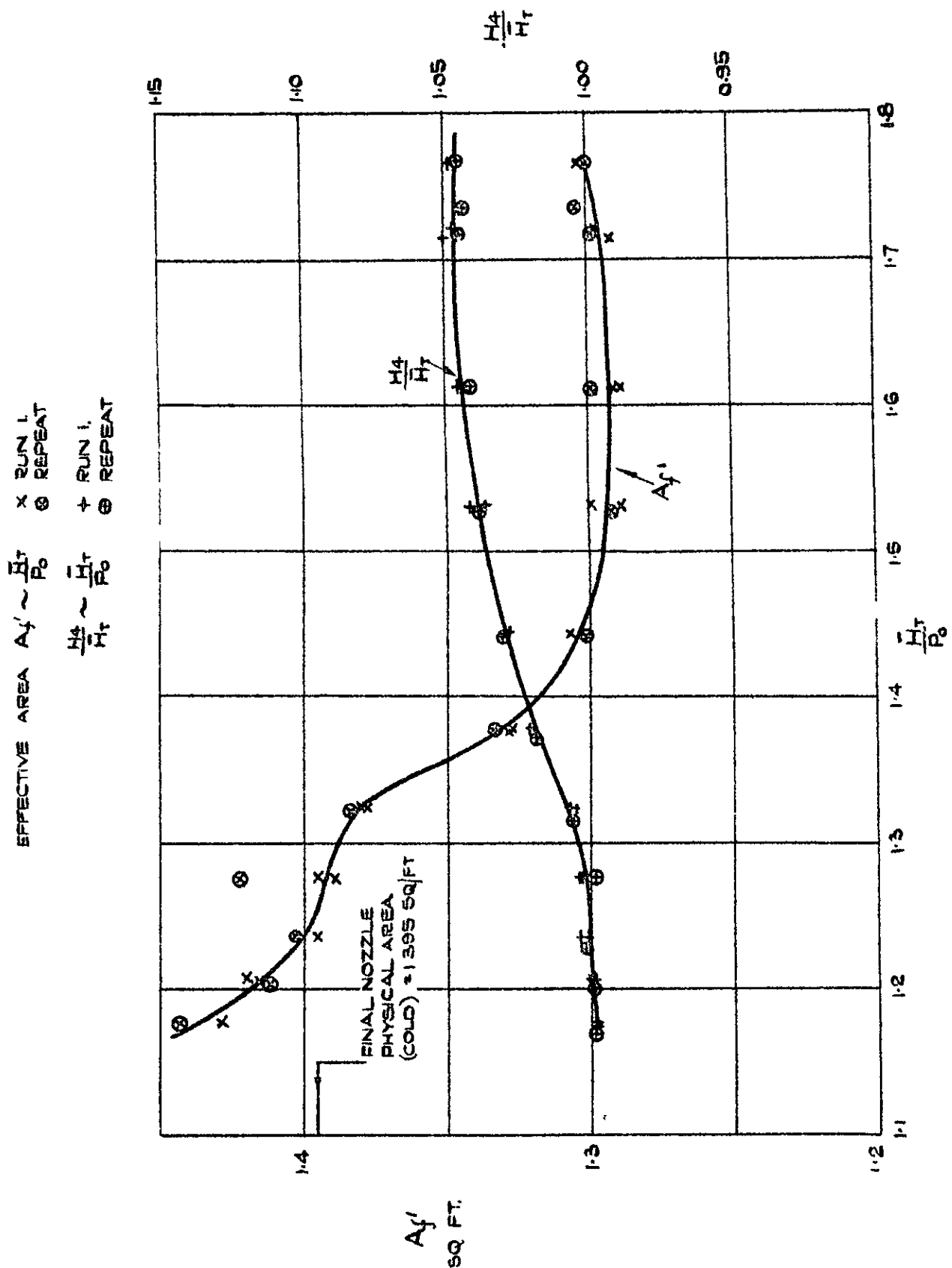
SINGLE PITOT TEST BED CALIBRATION.

FIG.4.
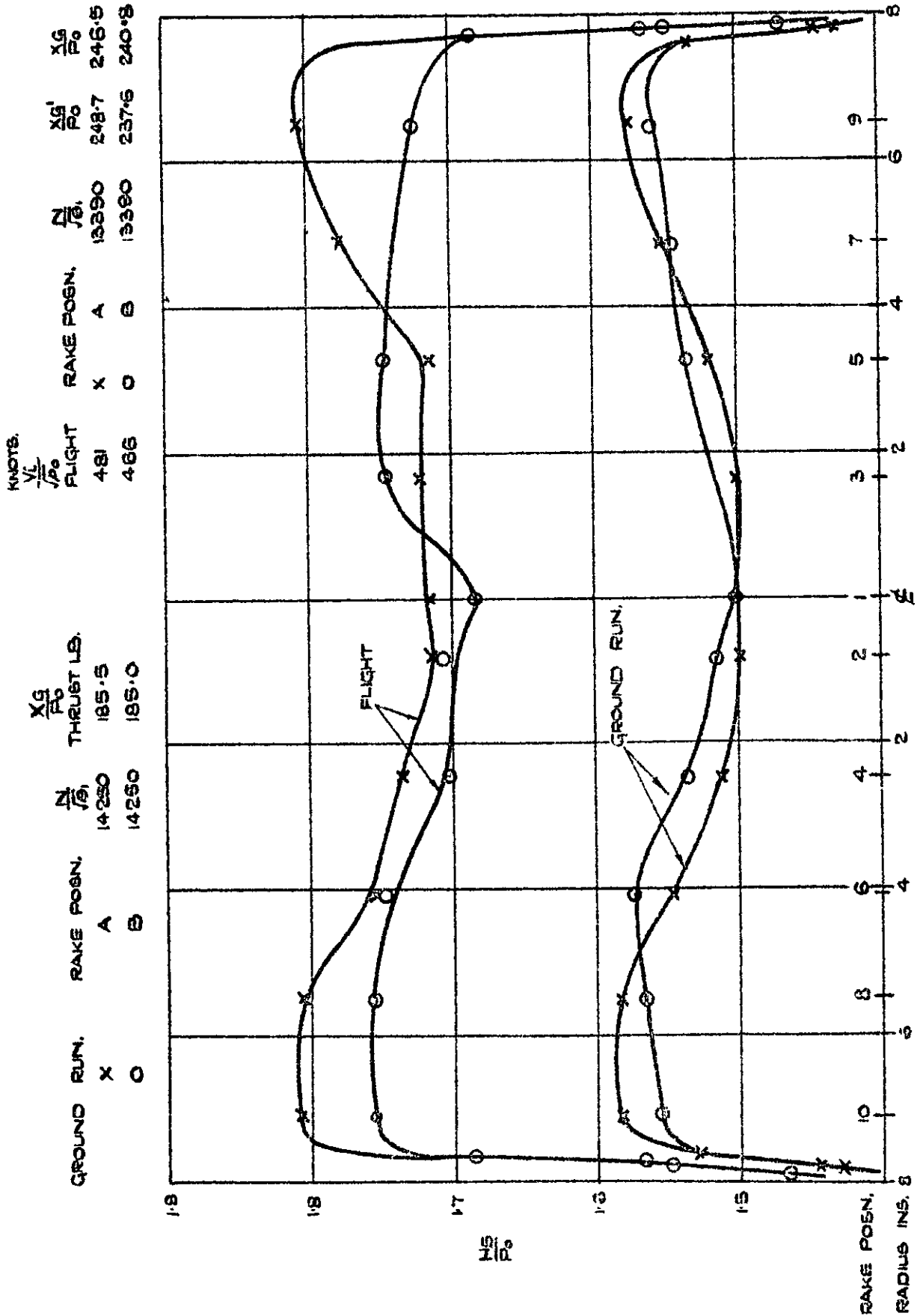
TYPICAL $\frac{H_6}{P_0}$ DISTRIBUTION ACROSS FINAL NOZZLE FOR GROUND RUN AND FLIGHT CASES.

FIG. 5.

RAKE POSITION		DATE
A	+	28.7.50
B	×	8.10.50
C	⊙	11.11.50
B'	⊙	8.12.50
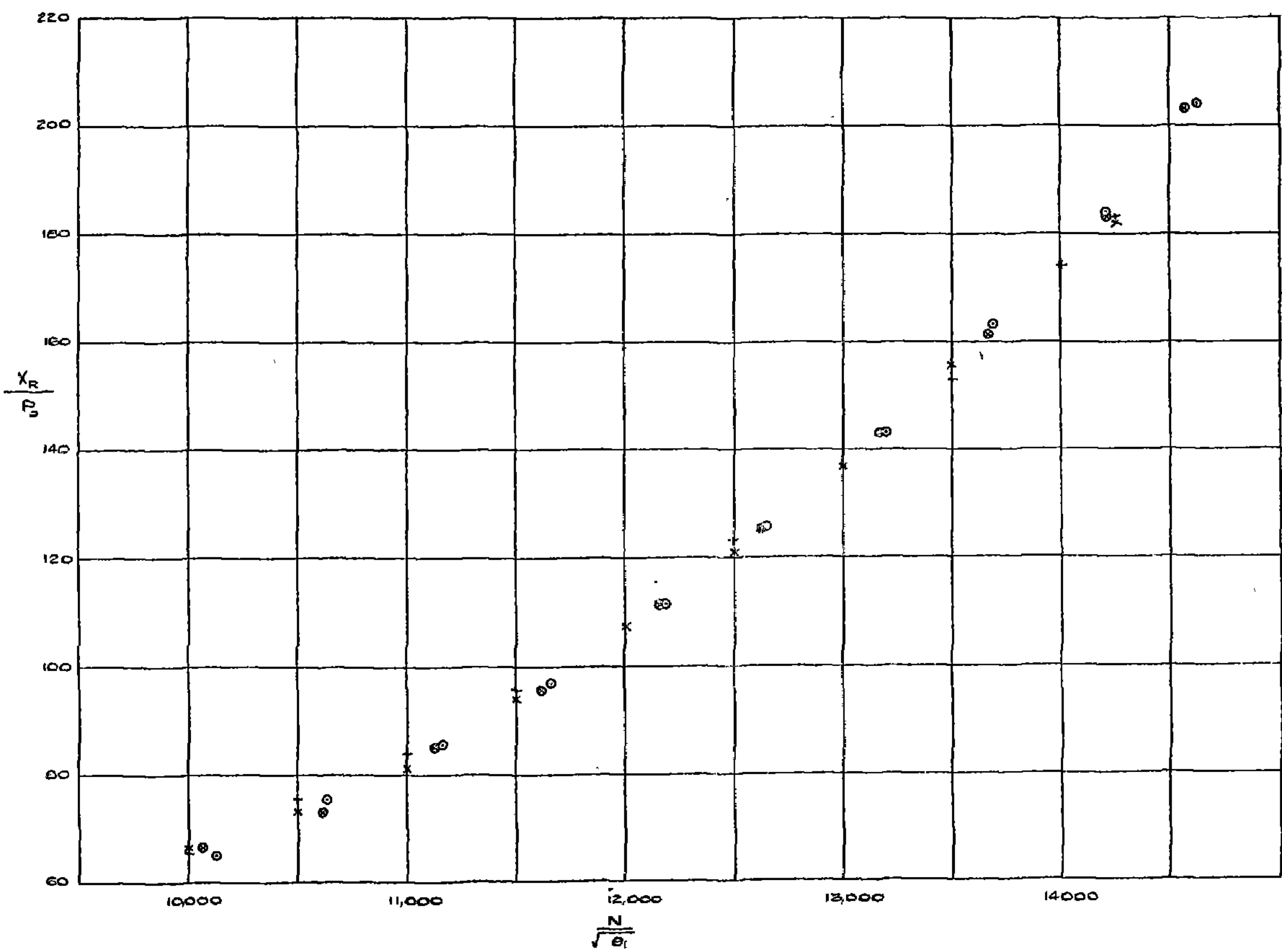
PLOT OF RAKE THRUST $\frac{X_R}{P_0}$ DURING GROUND RUN AGAINST $\frac{N}{\sqrt{\theta_1}}$ FOR THREE RAKE POSITIONS.

FIG. 6.
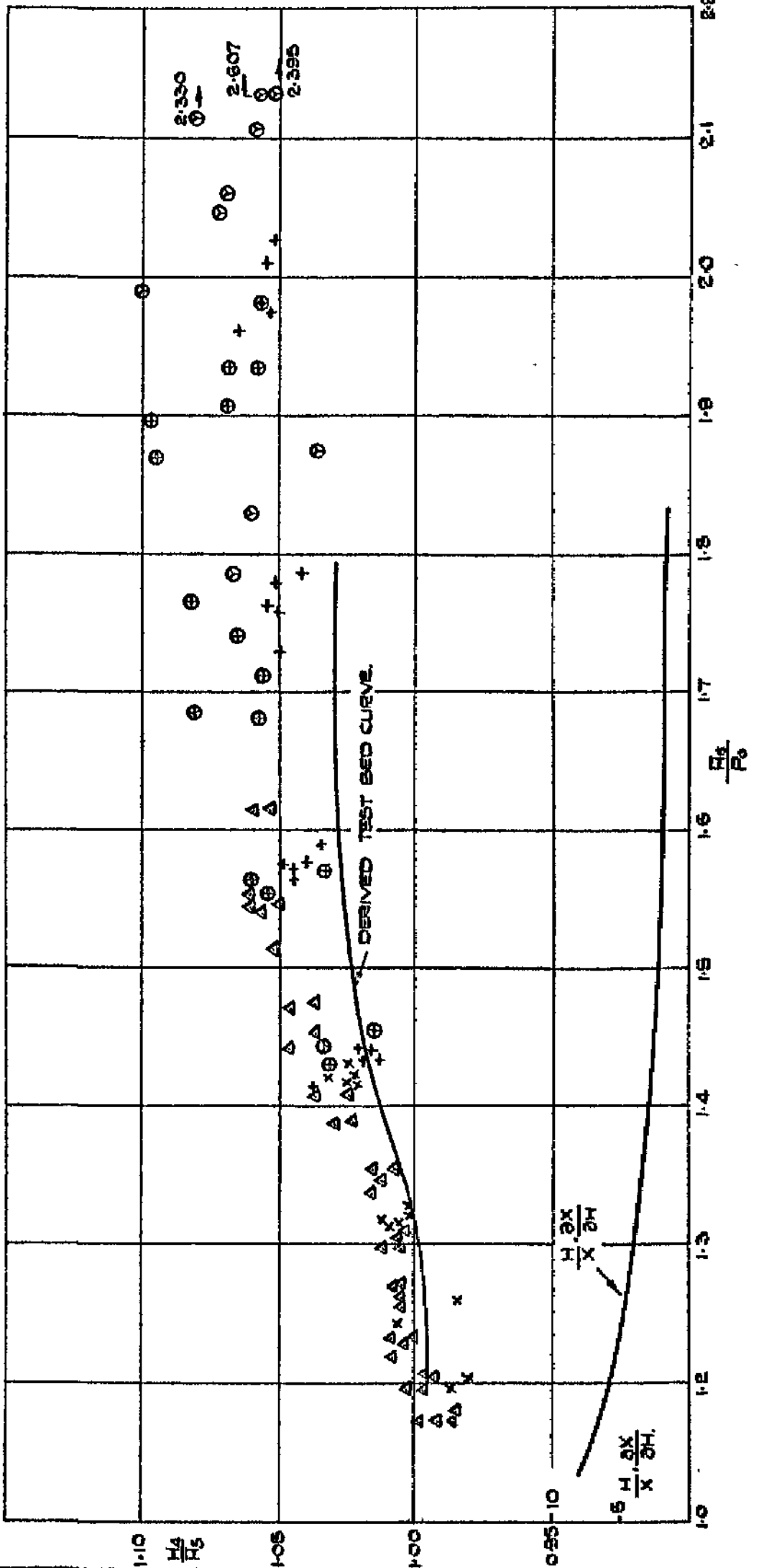
COMPARISON OF SINGLE PITOT AND MEAN RAKE TOTAL PRESSURE FOR ALL TESTS., ALSO DERIVATIVE $\dfrac{H}{X} \dfrac{\partial X}{\partial H}$

FIG. 7.
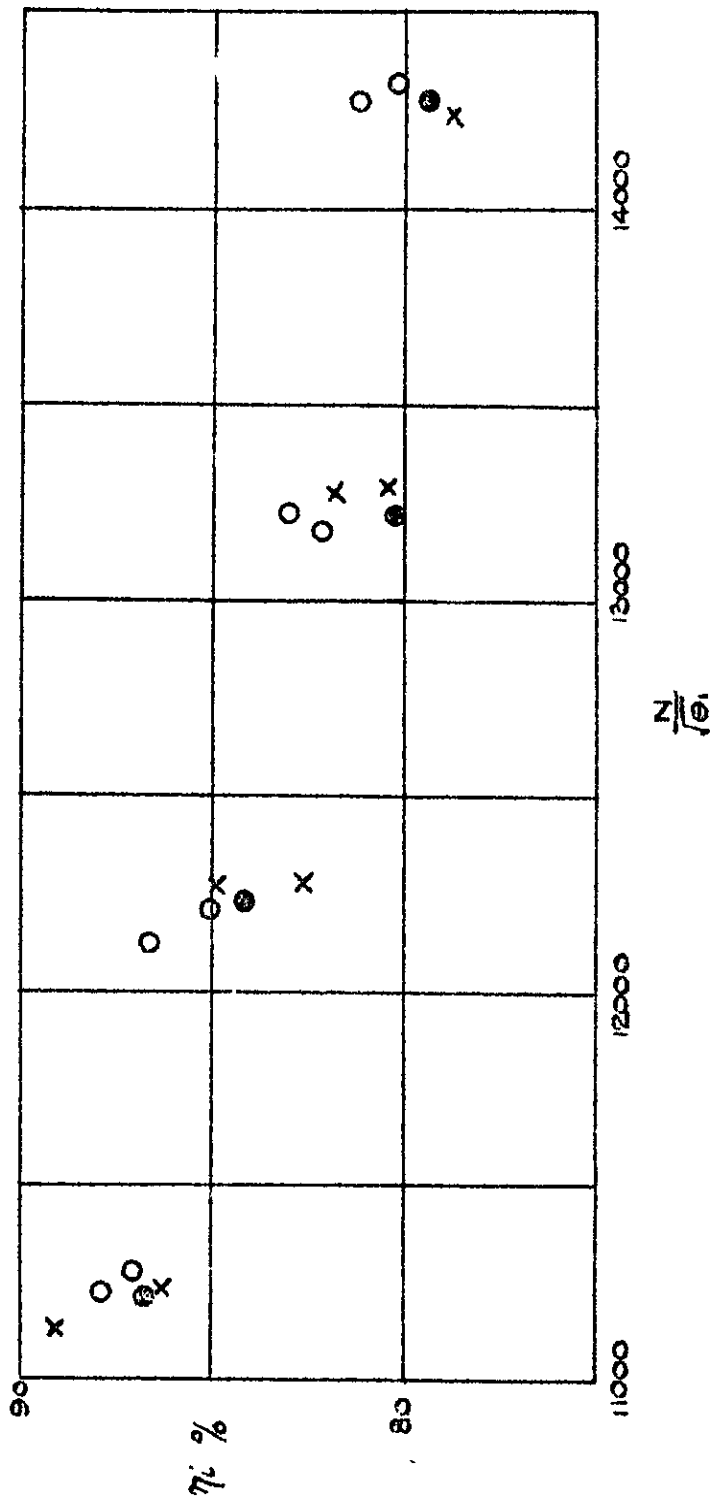
STARBOARD INTAKE EFFICIENCY. AT
5,000 AND 35,000 FEET. MACH № 0·62

FIG. 8.
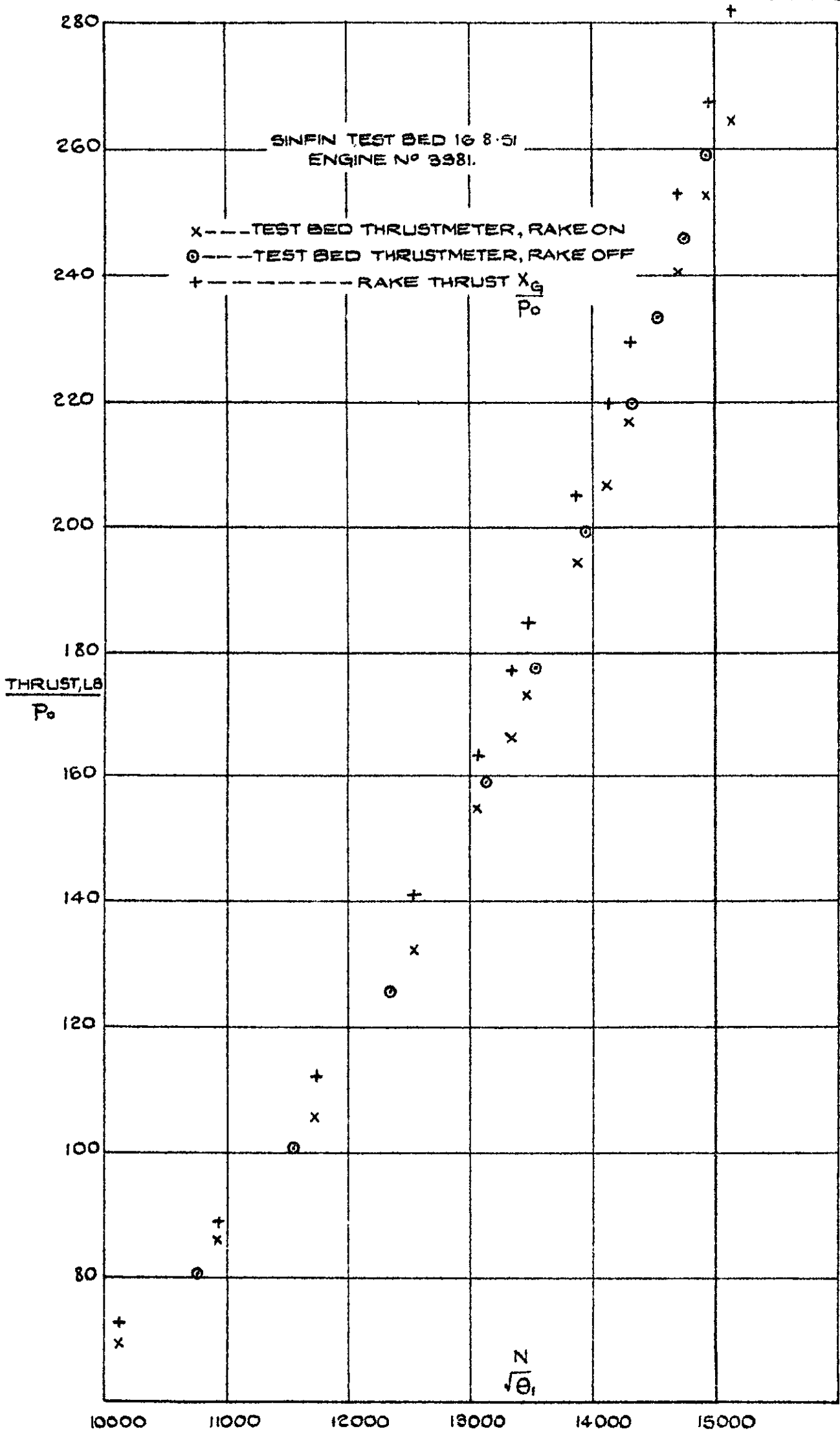
COMPARISON OF THRUSTS MEASURED ON TEST BED BY THRUSTMETER, AND
BY PITOT RAKE.

FIG. 9.

SINFIN TESTBED 16-8-51
DERWENT Ⅹ ENGINE N° 3381
SINGLE PITOT $\frac{H4}{Po}$ AND JET PIPE
TEMPERATURE ~ $\frac{N}{\sqrt{\theta_1}}$

X FLIGHT NOZZLE - RAKE ON
O FLIGHT NOZZLE - RAKE OFF

$\frac{H4}{Po}$

JET PIPE
TEMP ℃

$\frac{H4}{Po}$ →

JET PIPE
TEMPERATURE
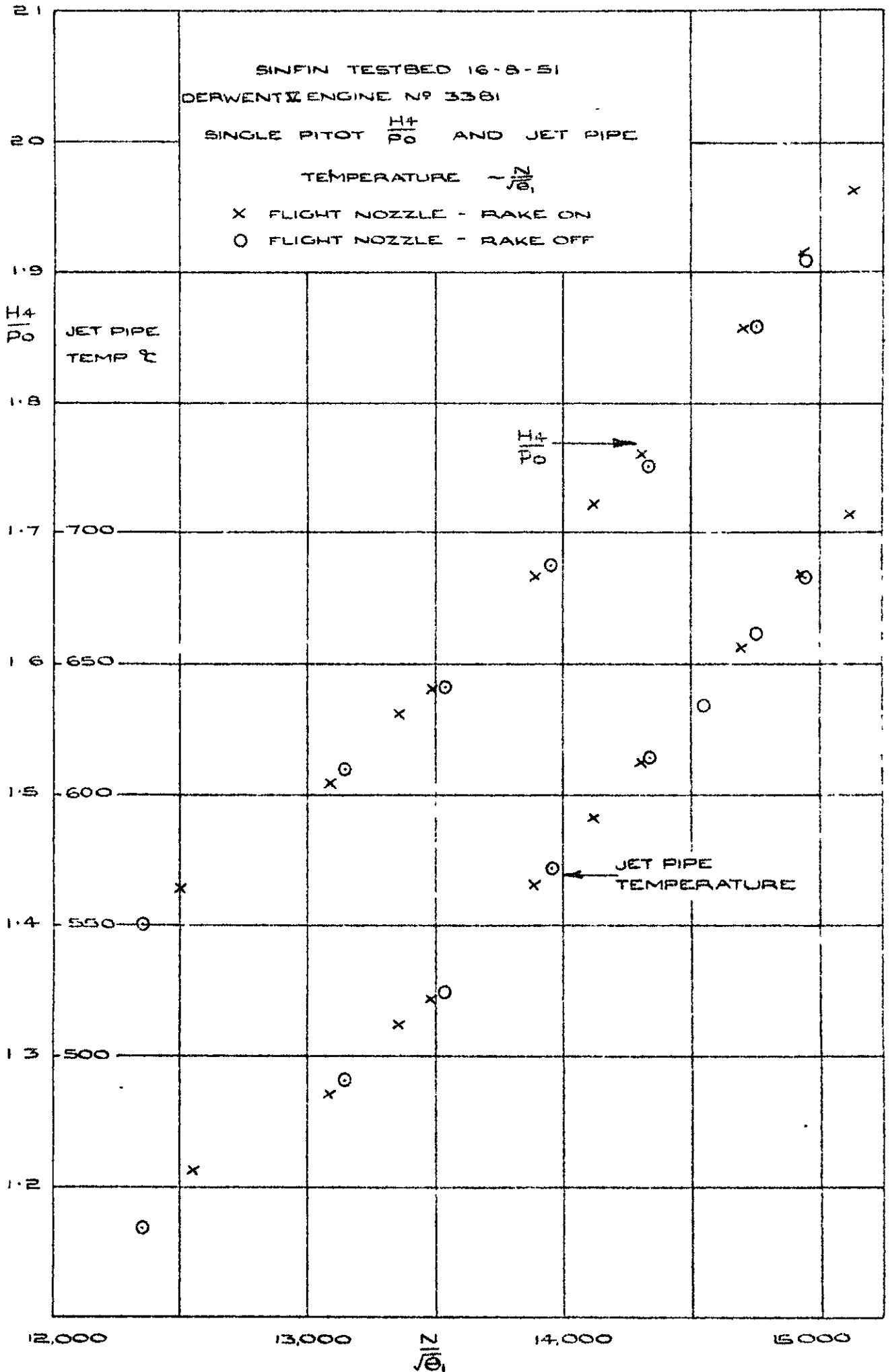
**EFFECT OF PRESENCE OF PITOT RAKE ON JET PIPE
TEMPERATURE & SINGLE PITOT. TEST BED RESULTS.**

FIG.13.

M		0·99	0·62	0·72
5,000FT	CENTRE STATIC	⊗	⊕	
	WALL STATIC	×	+	
35,000 FT & 40,000 FT	CENTRE STATIC		⊗	⊠
	WALL STATIC	Y	Y	Y

GROUND RUN	CENTRE STATIC	△
	WALL STATIC	*
TEST BED WALL STATIC		O

THEORETICAL VALUE ABOVE CHOKE

$\frac{\overline{H_5}}{P_0}$

$\frac{P_3 - P_0}{\overline{H_5} - P_0}$
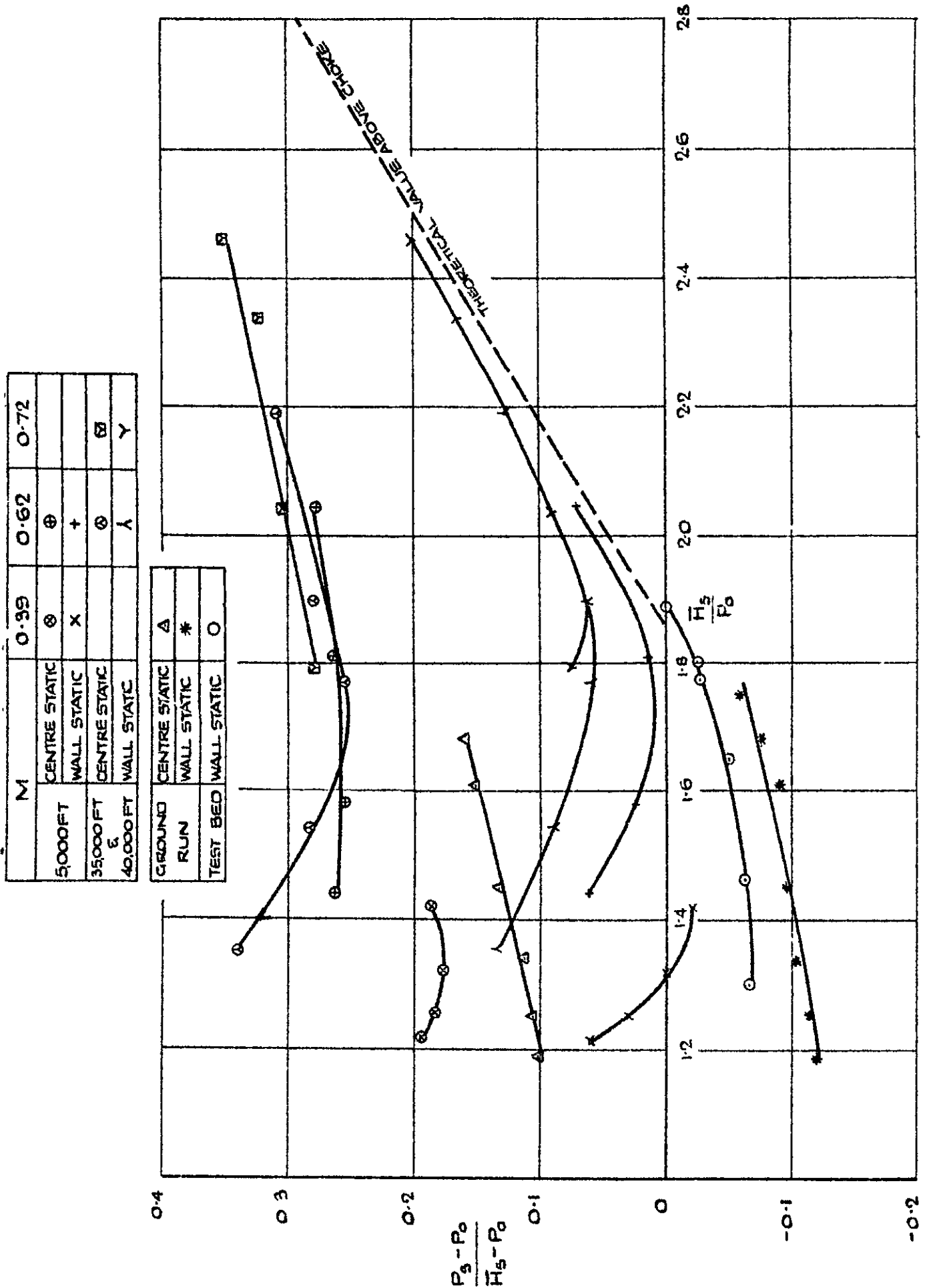
FINAL NOZZLE CENTRE & WALL STATIC PRESSURES—
FLIGHT, GROUND RUN AND TEST BED RESULTS.

FIG.14.
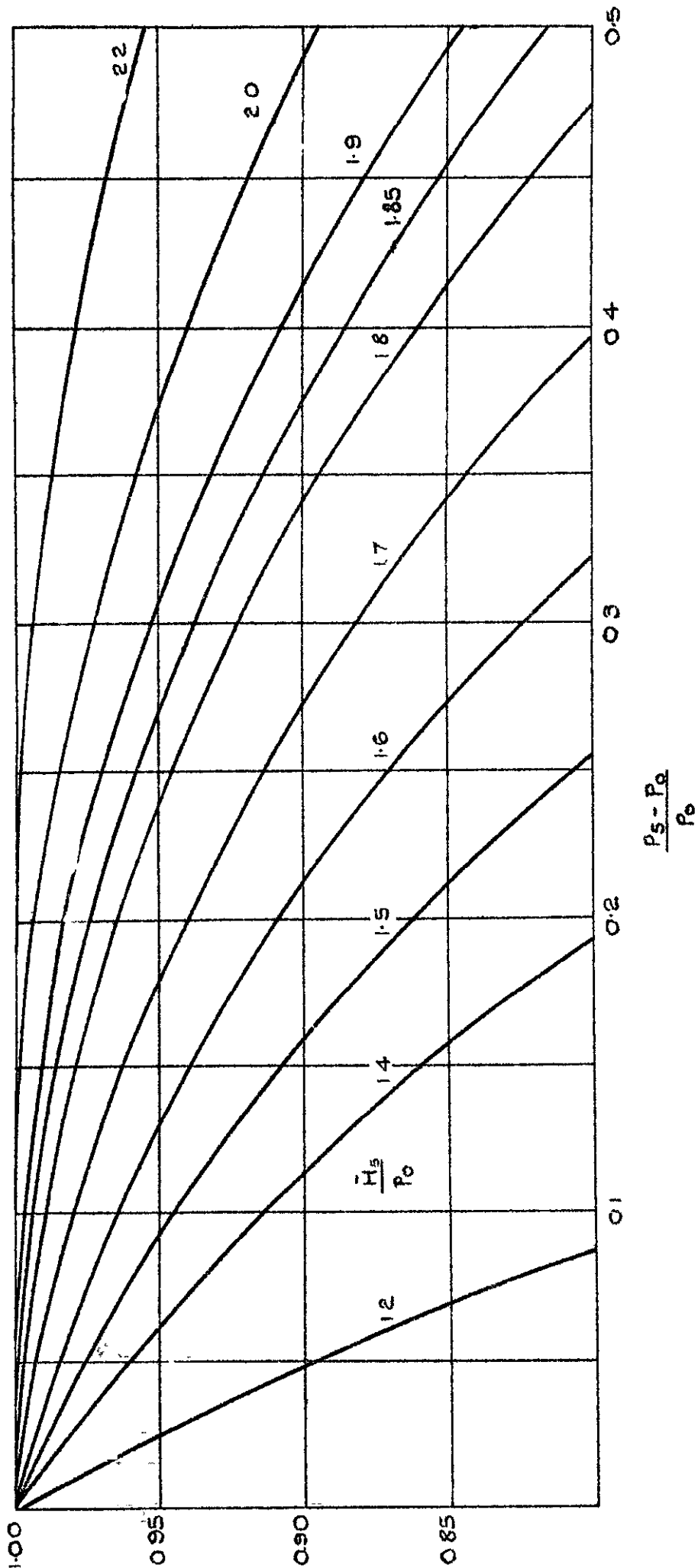
EFFECT OF DEPARTURE IN EXIT STATIC PRESSURE FROM CONVENTIONALLY
ASSUMED VALUE ON THRUST ESTIMATED DIRECT FROM JET PIPE TOTAL
PRESSURE.

	HEIGHT	MACH N°
X	GROUND RUN.	———
△	5,000 FT.	0.39
+	5,000 FT.	0.62
O	35,000 FT & 40,000 FT.	0.62
▽	35,000 FT & 40,000 FT	0.72

PERCENTAGE
CORRECTION
TO

−5

RAKE THRUST
FOR STATIC
PRESSURE.

1.0   1.2   1.4   1.6   1.8   2.0   2.2   2.4   2.6   2.8

$\dfrac{P_3}{P_0}$

FIG.15.

FIG.16.
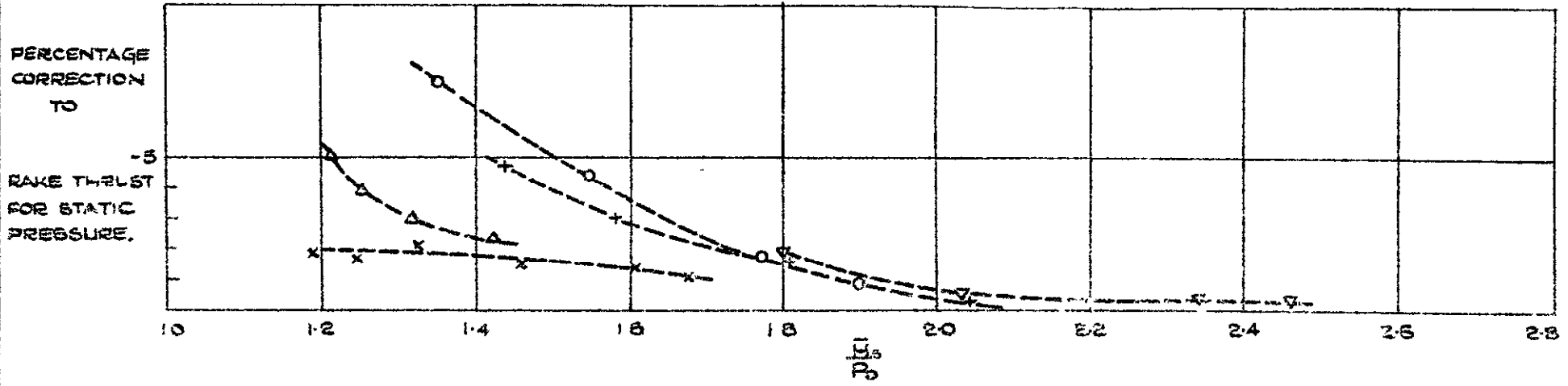
GROUND RUN △

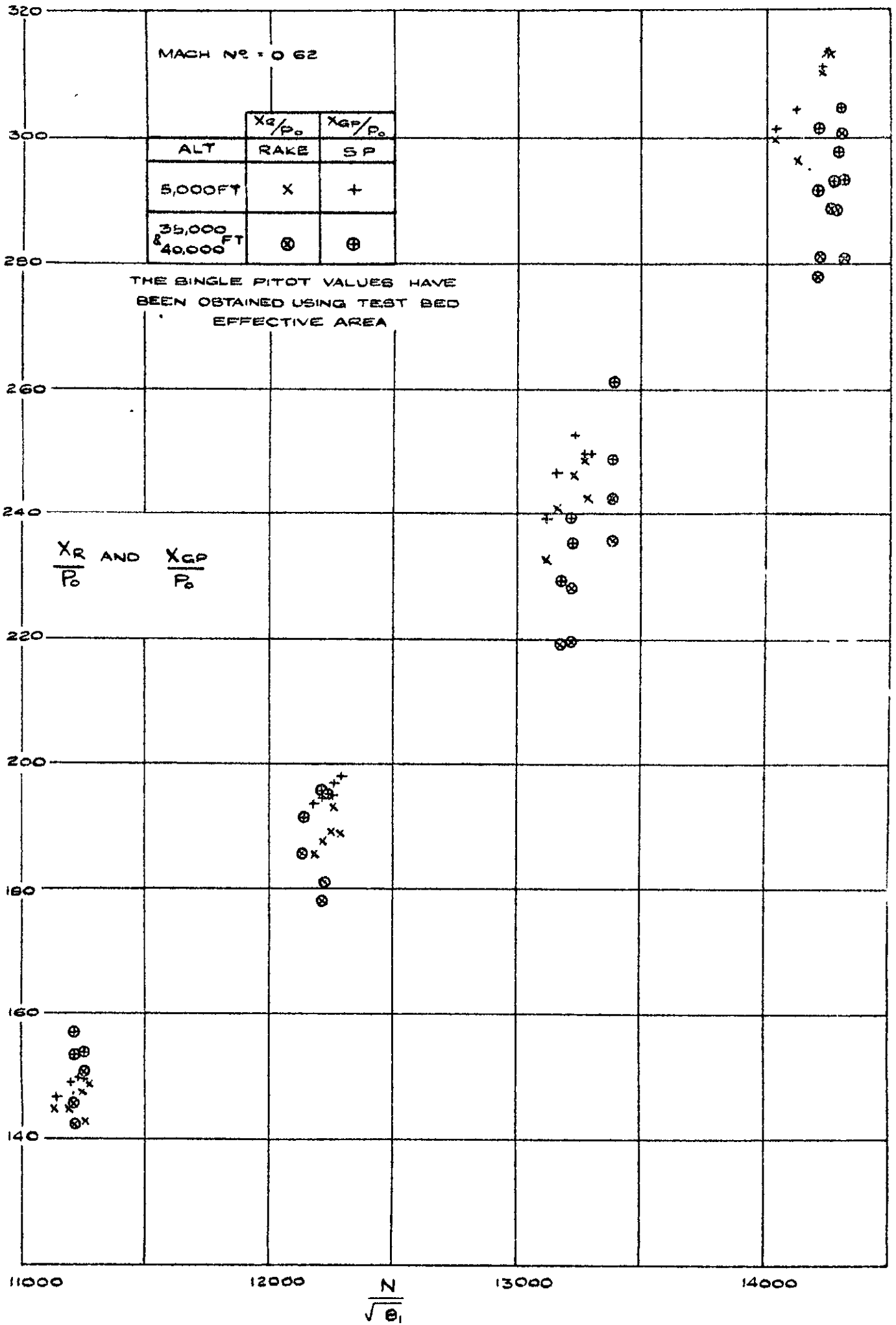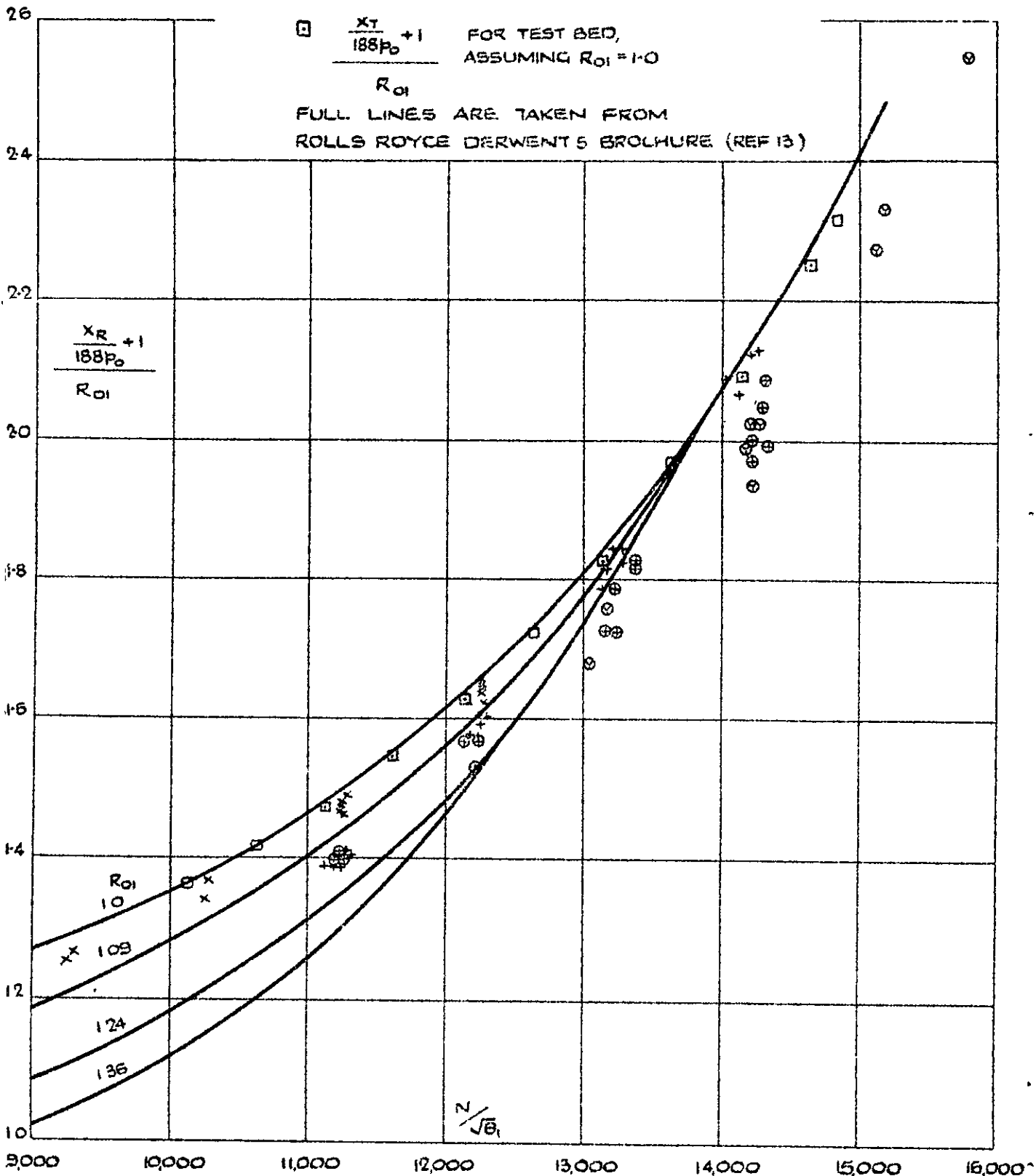| MACH Nº	0·39	0·62	0·72
5,000 FT.	×	+	
35,000 & 40,000 FT.		⊕	⊗
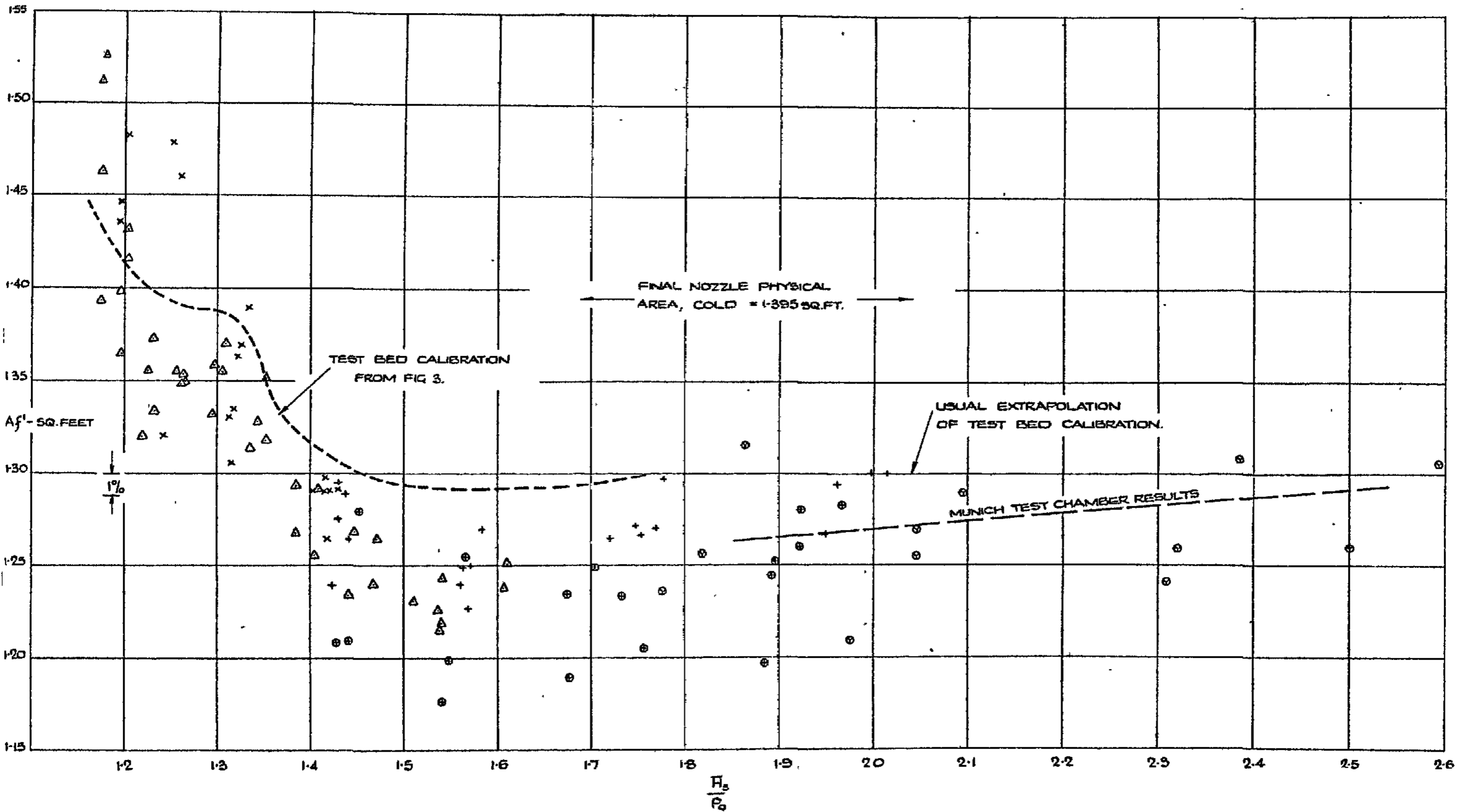
FINAL NOZZLE EFFECTIVE AREA A𝒇' OBTAINED FROM CALIBRATION OF SINGLE PITOT AGAINST THRUSTMETER ON TEST BED, AND AGAINST RAKE ON GROUND AND IN FLIGHT PLOTTED AGAINST $\overline{H_s}/P_0$

FIG.17.

MACH Nº	0·39	0·62	0·72
5000 FT	×	+	
35000FT & 40,000 FT.		⊕	⊘
GROUND RUN. △			
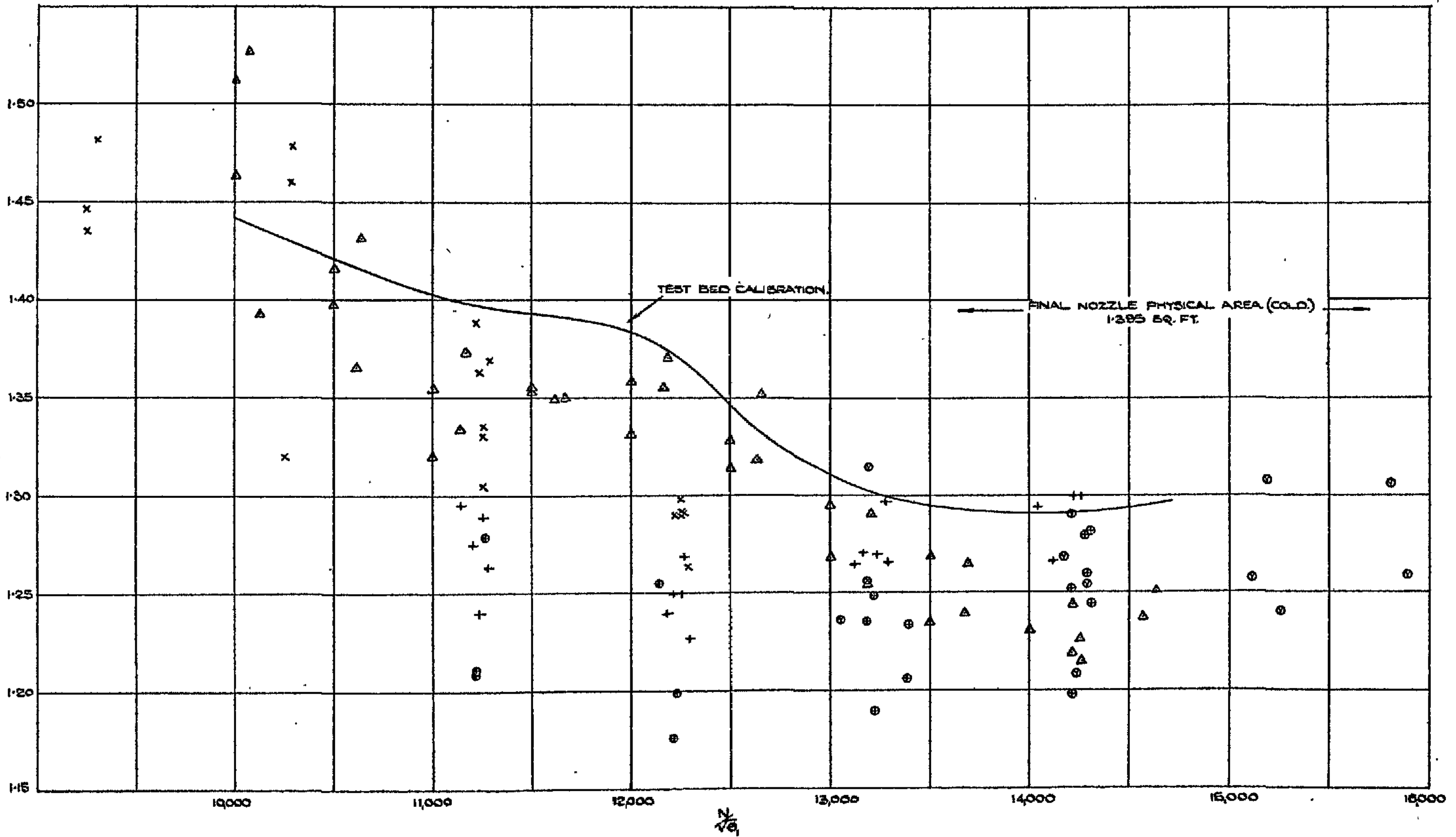
FINAL NOZZLE EFFECTIVE AREA A$_f$ OBTAINED FROM CALIBRATION OF SINGLE PITOT AGAINST THRUSTMETER ON TEST BED, & AGAINST RAKE ON GROUND AND IN FLIGHT. PLOTTED AGAINST N/√θ

FIG.18.

FLIGHT THRUST MEASURED BY RAKE $\frac{X_R}{P_0}$ AND BY SINGLE PITOT $\frac{X_{GP}}{P_0}$ AT 5,000 FT.
AND 35,000 FT AT MACH. N⁰ = 0·62 PLOTTED AGAINST $\frac{N}{\sqrt{\theta_1}}$

FIG.19.

MACH Nº	0 39	0 62	0 72
RAM RATIO	1·09	1·24	1 36
5,000 FT	×	+	
35,000 & 40,000 FT		⊕	⊗

ALL FLIGHT RESULTS INCLUDED

☐ $\dfrac{\dfrac{X_T}{188P_o}+1}{R_{OI}}$ FOR TEST BED, ASSUMING $R_{OI}=1\cdot0$

FULL LINES ARE TAKEN FROM ROLLS ROYCE DERWENT 5 BROCHURE (REF 13)

$\dfrac{\dfrac{X_R}{188P_o}+1}{R_{OI}}$

$\dfrac{N}{\sqrt{\theta_1}}$

PLOT OF $\dfrac{\dfrac{X_R}{188P_o}+1}{R_{OI}}$ AGAINST $\dfrac{N}{\sqrt{\theta_1}}$ FOR FLIGHT MEASUREMENTS, & COMPARISON WITH TEST BED, THRUSTMETER AND BROCHURE FIGURES.